The 53th Fluid Dynamics Conference/ The 39th Aerospace Numerical Simulation Symposium
30th June 2021

APC-7の集計結果
Summary of APC-7

橋本 敦 (JAXA) , APC有識者会議
Hashimoto Atsushi(JAXA), APC committee

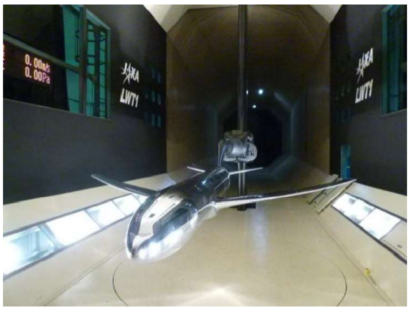

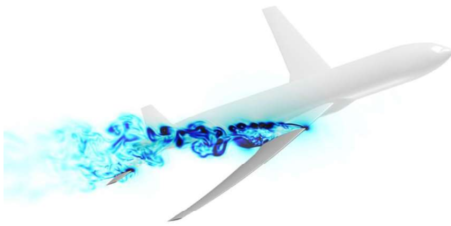

Statistics of submitted data

- Organizations and number of submitted data(total 23 data)
  - National research institutes：JAXA(11)
  - Universities: Univ. of Tokyo(6), YNU(3), Iwate Univ.(1)
  - Aerospace industries: KHI(2)
- Grids
  - JAXA：5
  - Customs：5
- Code
  - Unstructured solver(16)
  - Cartesian solver(7)
- Turbulence models
  - Steady: SA(7), SST(3)
  - Unsteady: SA(8), SST(3), ILES(2)
- Initial conditions
  - Steady: Uniform flow(10)
  - Unsteady: Uniform flow(4), Restart from the steady-state solution(8), Mapping(1)

Participants of case 1

ID	Name	Organization	Code	Grid	Turbulence Model	Initial Condition	Note
A1	橋本敦	JAXA	FaSTAR（Unstructured solver）	BOXFUN	SST-2003	Uniform flow	Hanging node
A2				UPACS	SA-noft2-R		
A3					SST-2003		
A4				MEGG3D	SA-noft2-R		
A5					SST-2003		
B1	上野 陽亮	川崎重工	Cflow（Unstructured solver）	Custom（Orthogonal octree + Body-Fitted layer grid）	SA-neg	Uniform flow	Local time step
B2							Global time step
C1	原惇	東京大学	UTCart（Cartesian solver）	Custom（Orthogonal grid）	SA-noft2-R (Crot=1)	Uniform flow	Grid #1（Number of cells is 140M）
C2				Custom（Orthogonal grid）			Grid #2（Number of cells is 90M）
D1	菅谷圭祐	東京大学	UTCart（Cartesian solver）	Custom（Orthogonal grid）	SA-noft2-R (Crot=1)	Uniform flow	

3

Participants of case 2

ID	Name	Organization	Code	Grid	Turbulence Model	Initial Condition	Note
A1	橋本敦	JAXA	FaSTAR（Unstructured solver）	BOXFUN	SST-2003 IDDES	Restart from the steady-state solution	Hanging node
A2				UPACS	SA-noft2-R IDDES		
A3					SST-2003 IDDES		
A4				MEGG3D	SA-noft2-R IDDES		
A5					SST-2003 IDDES		
C1	原惇	東京大学	UTCart（Cartesian solver）	Custom（Orthogonal grid）	SA-noft2-R (Crot=1)	RANSの収束解からリスタート	Grid #1（Number of cells is 140M）
C2				Custom（Orthogonal grid）			Grid #2（Number of cells is 90M）
D1	菅谷圭祐	東京大学	UTCart（Cartesian solver）	Custom（Orthogonal grid）	DDES-protected (SA-noft2-R Crot=1)	RANSの収束解からリスタート	
E1	坂井玲太郎	JAXA	LS-FLOW-HO（Unstructured solver）	Custom（Hexa second order element）	ILES	同じ迎角の「4次精度・wall-model無し」の解からマッピング	
F1	髙橋佑太	岩手大学	Cut-Cell Iwate（Cartesian solver）	Custom（Orthogonal grid）	ILES+Wall model	Uniform flow	
G1	安村祐哉	横浜国立大学	FaSTAR（Unstructured solver）	HexaGrid	SA-noft2-R DDES (Cdes = 0.51, Crot = 2.0)	Uniform flow	HR-SLAU2
G2					SA-noft2-R DDES (Cdes = 0.65, Crot = 1.0)		HR-SLAU2
G3					SA-noft2-R DDES (Cdes = 0.65, Crot = 1.0)		SLAU2

4

Surface grid(Wing root)

BO=BOXFUN
UP=UPACS
ME=MEGG3D
He=HexaGrid
Cu=Custom

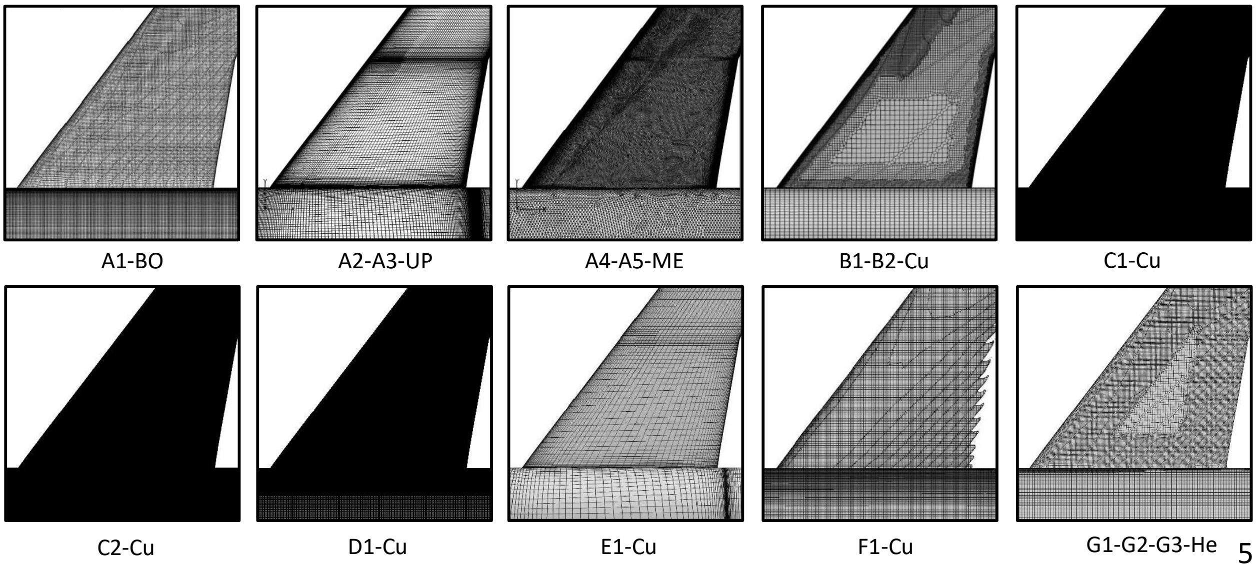

5

Surface grid(Wing root)

BO=BOXFUN
UP=UPACS
ME=MEGG3D
He=HexaGrid
Cu=Custom

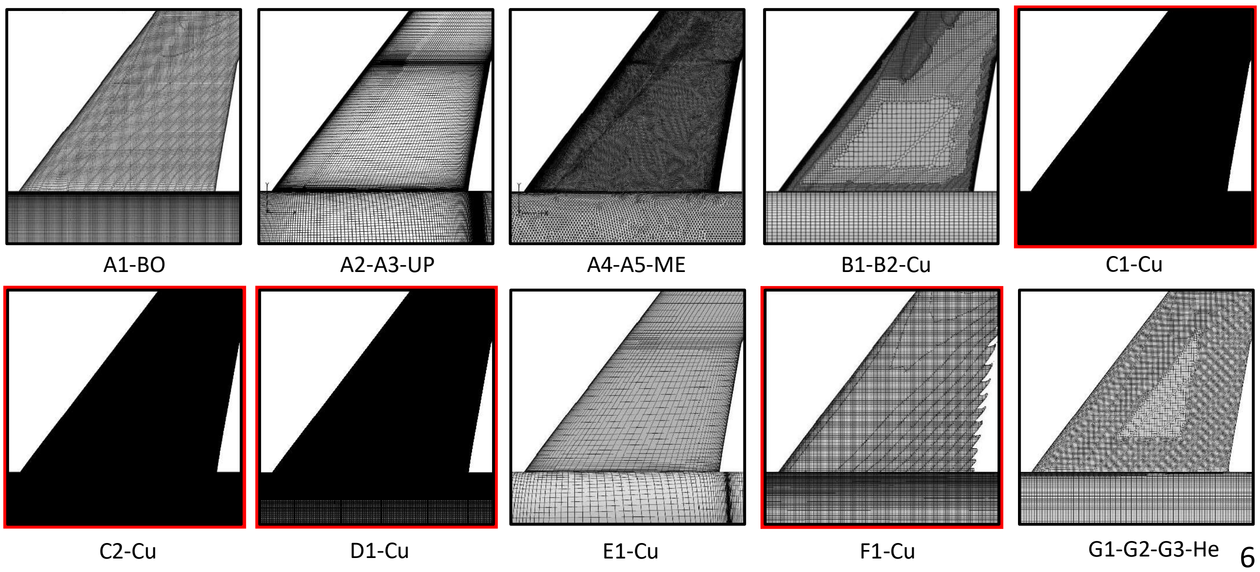

6

Cartesian

Surface grid(Wing root)

Hexahedral unstructured

BO=BOXFUN
UP=UPACS
ME=MEGG3D
He=HexaGrid
Cu=Custom

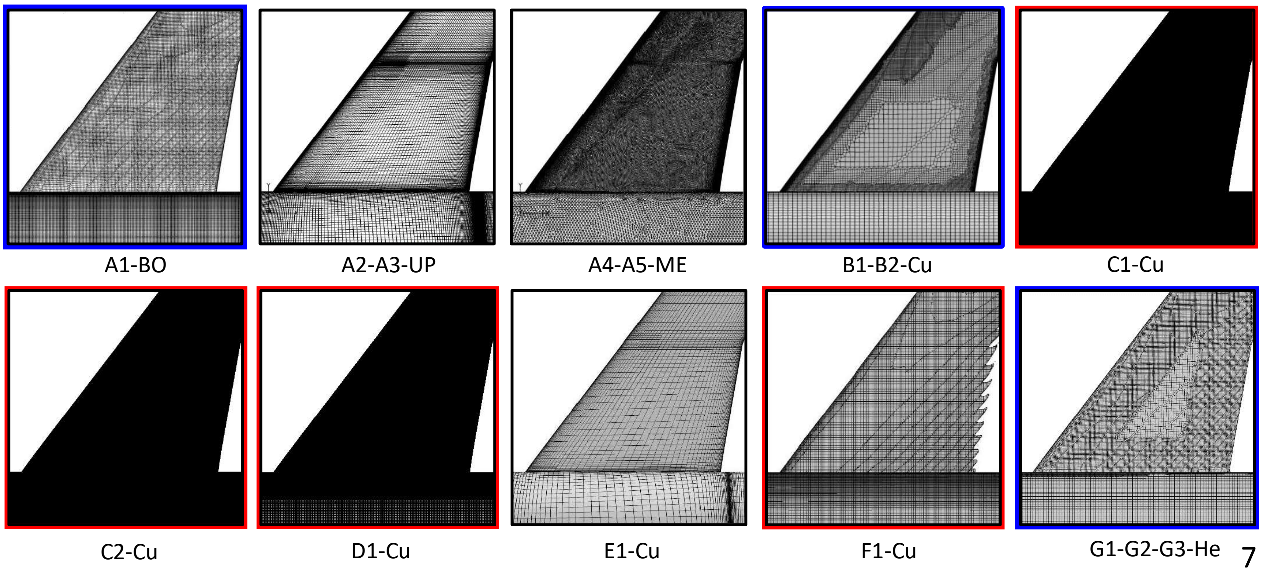

7

Cartesian

Surface grid(Wing root)

Hexahedral unstructured

Mixed-element unstructured (Tetra,Prism,Pyramid,Hexa)

BO=BOXFUN
UP=UPACS
ME=MEGG3D
He=HexaGrid
Cu=Custom

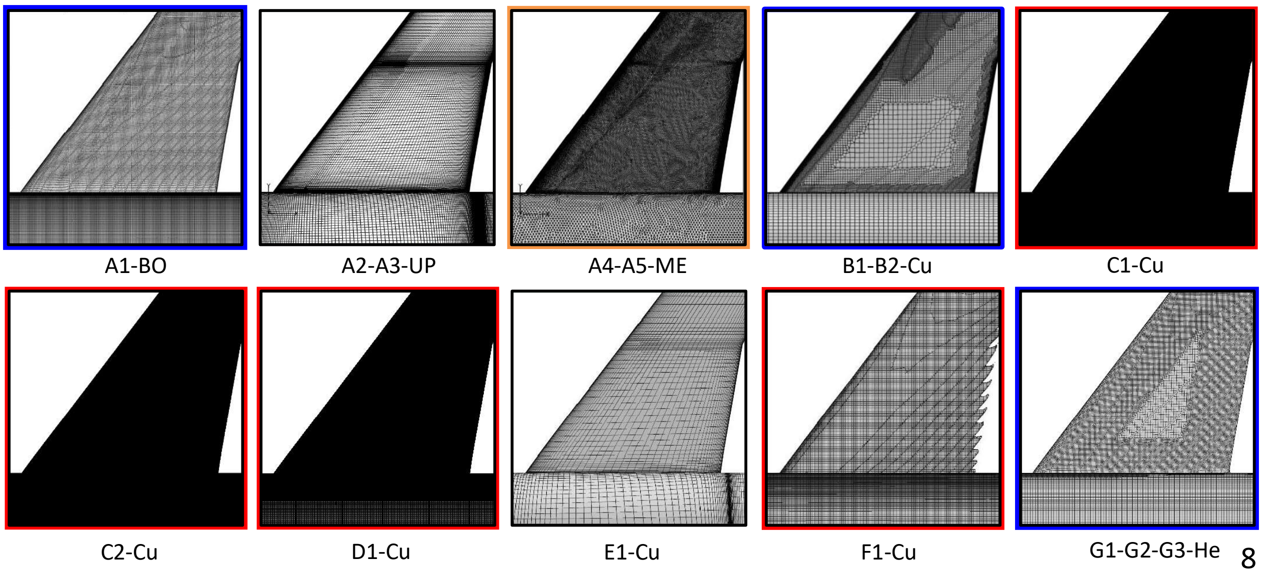

8

Cartesian

Surface grid(Wing root)

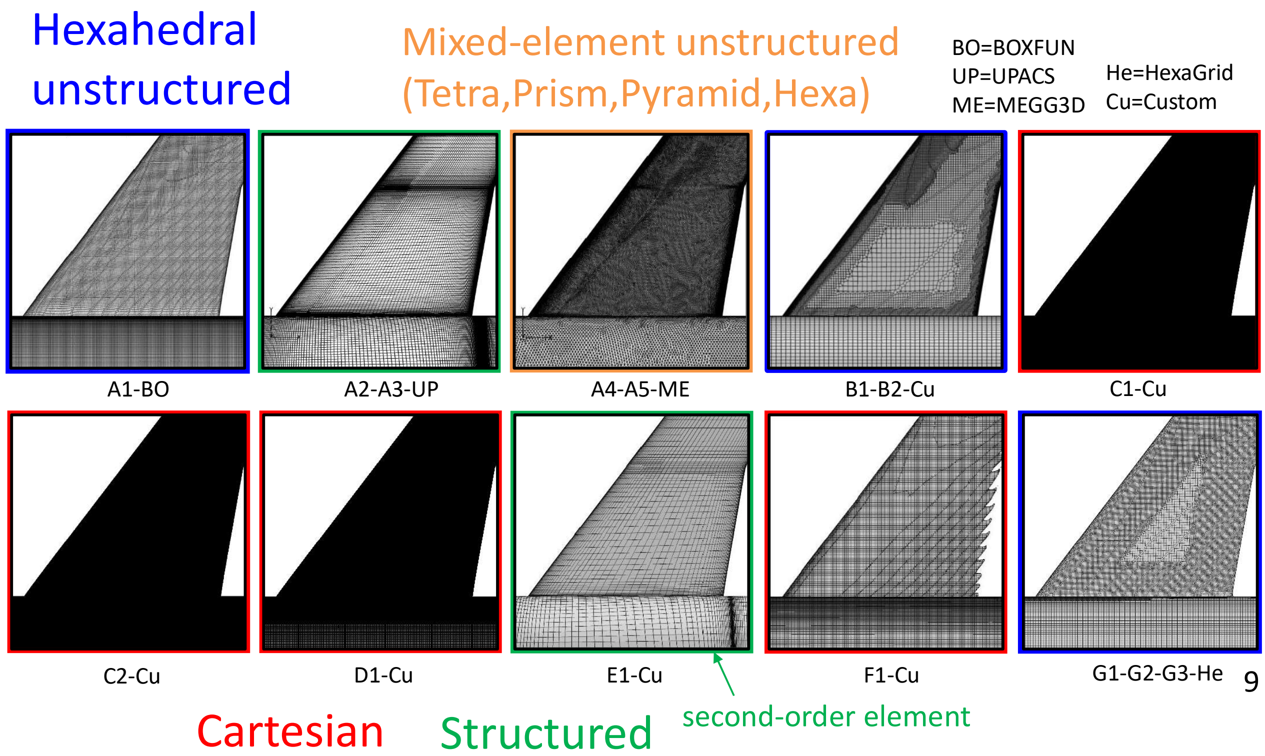

Surface grid(Tail)

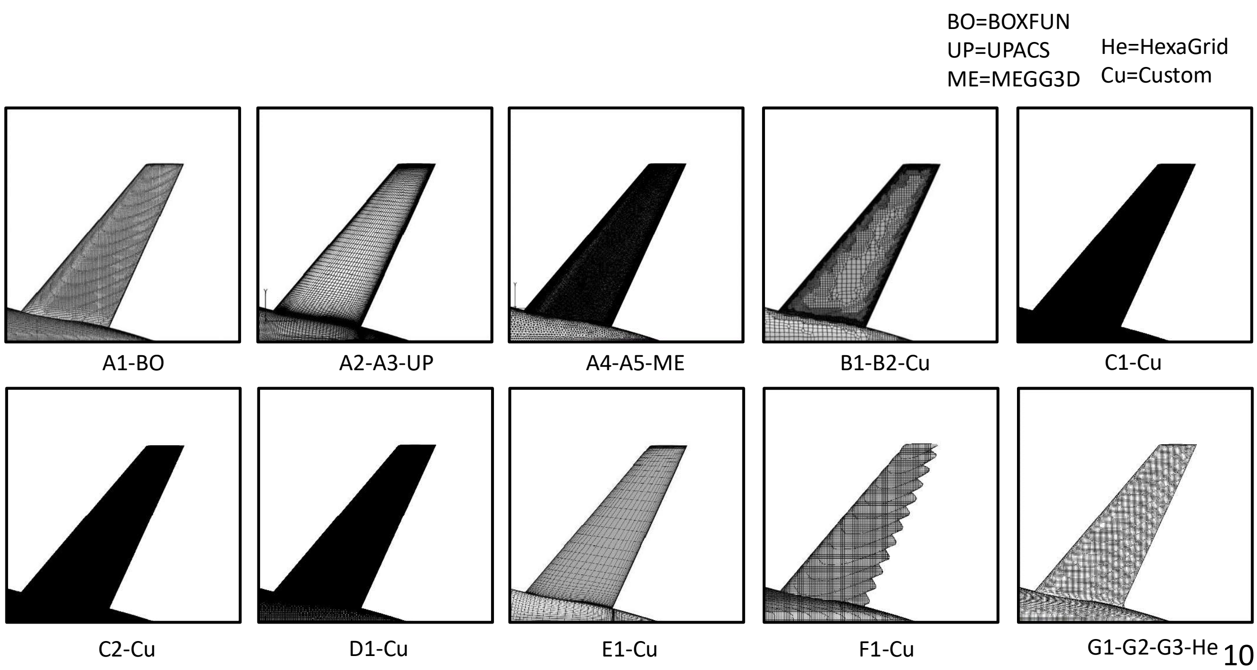

Cross section grid

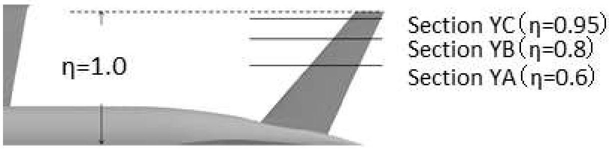

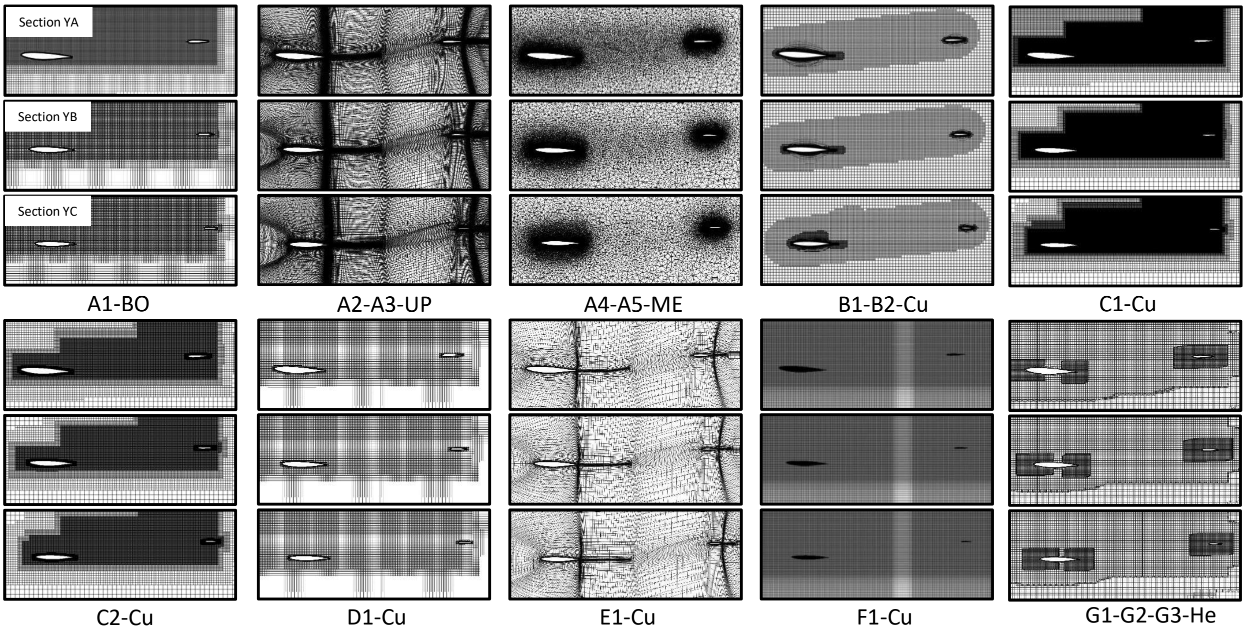

11

Case1 : Steady computation

- Aims
  - Understand the prediction accuracy of aerodynamic performance such as CL, CD, Cm at low speeds and separation characteristics (beginning of separation, separated area).
  - Understand the dependency of turbulence model, grid.

- Conditions
  - M = 0.168, Re_c = 1.06 x 10^6, T_{ref}=310K
  - AoA = -3.22, -0.67, 2.89, 5.95, 9.01, 10.03, 11.05, 12.06, 13.08, 14.08, 18.08deg

12

CL-Alpha, case1

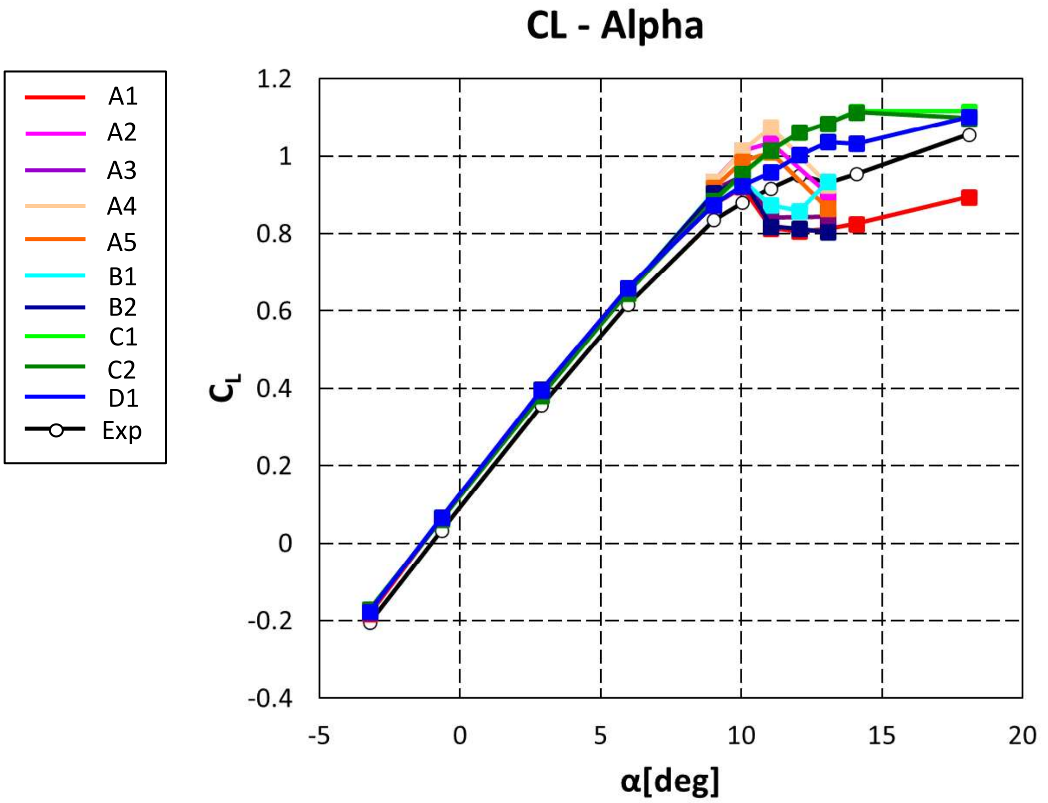

13

CL-Alpha, case1

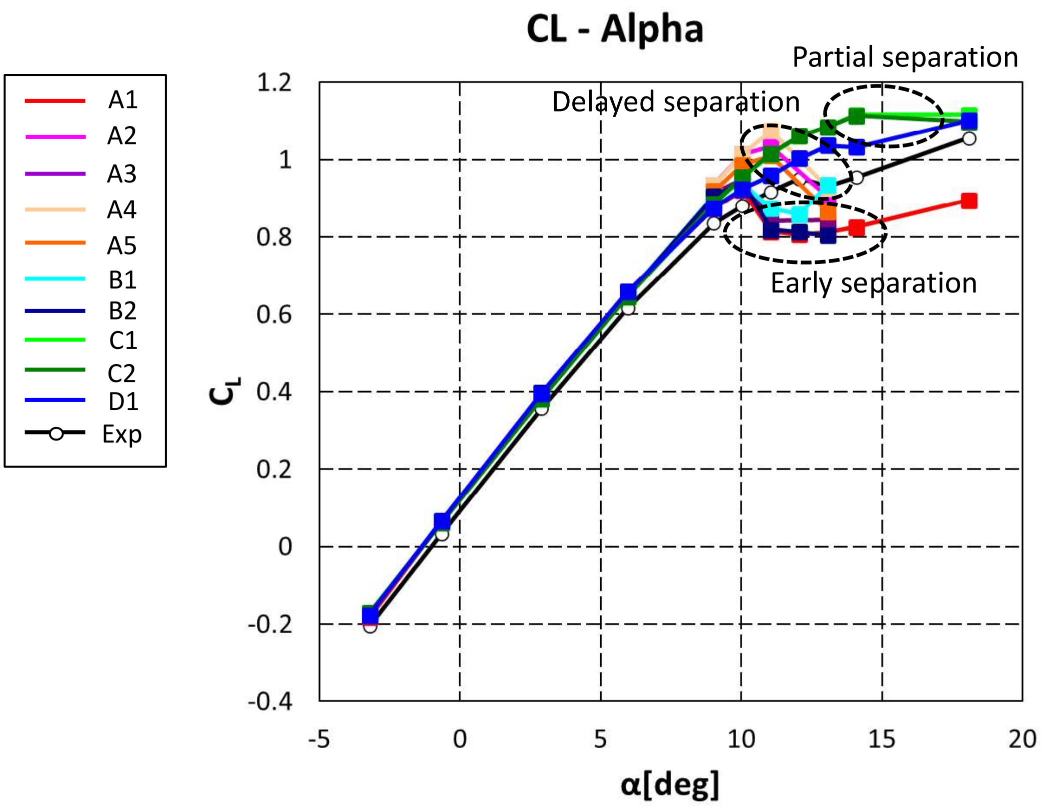

14

CD-Alpha，case1

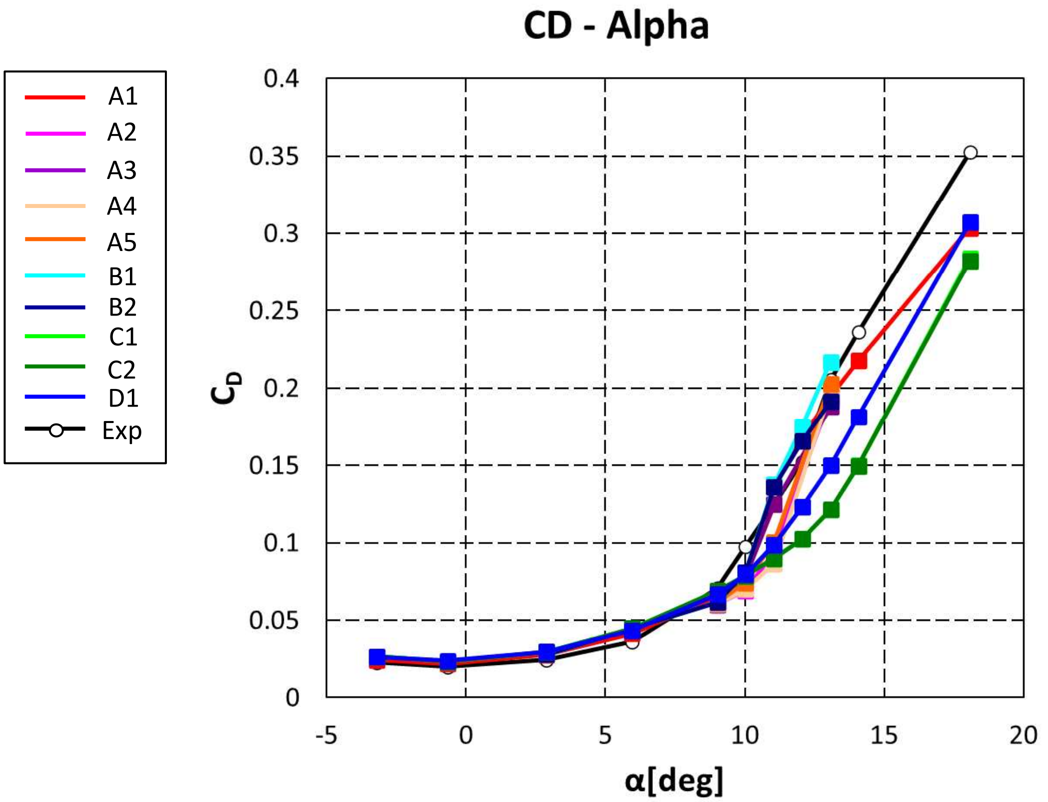

15

Cm-Alpha，case1

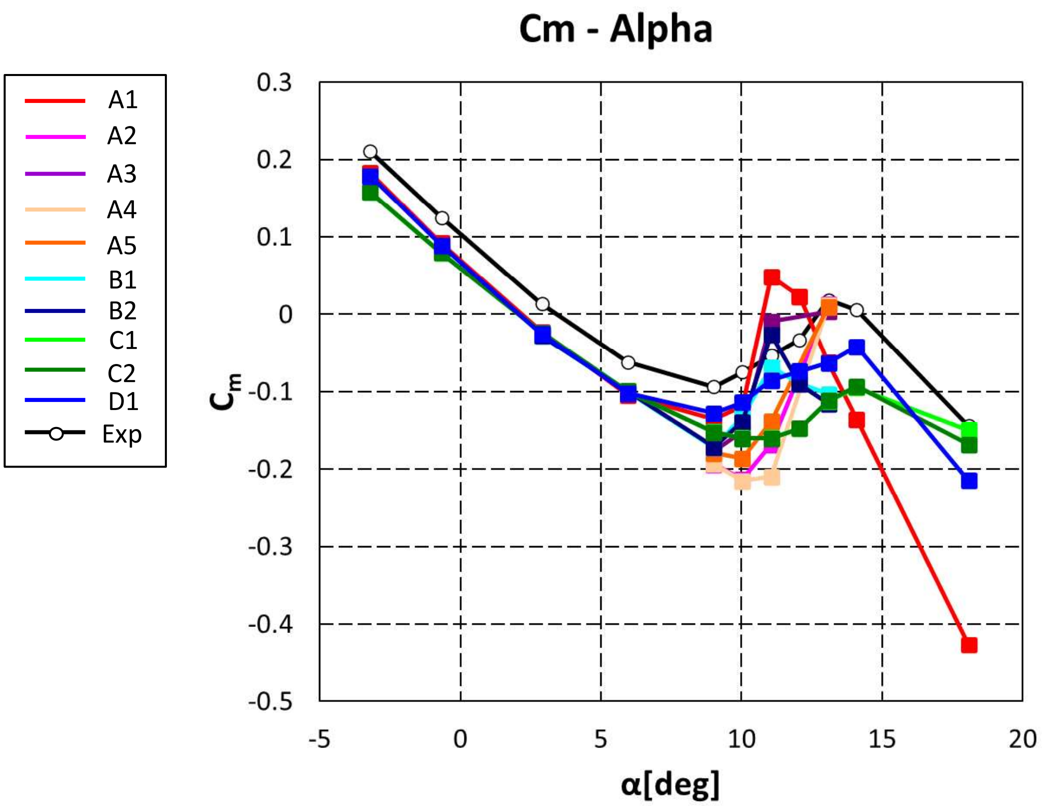

16

Surface streamline(11.05deg)

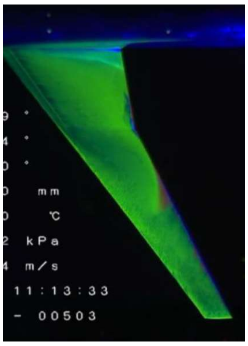

The flow tends to separate for hexahedral unstructured grid and SST model

T. Uchiyama, et al., AIAA 2019-2190

CL-Alpha

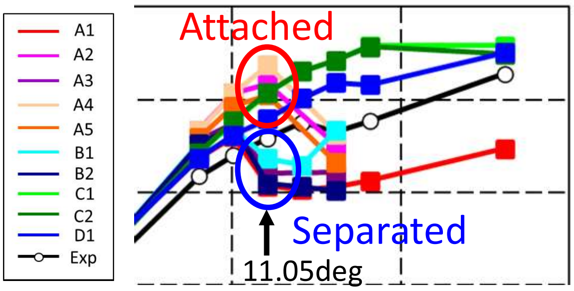

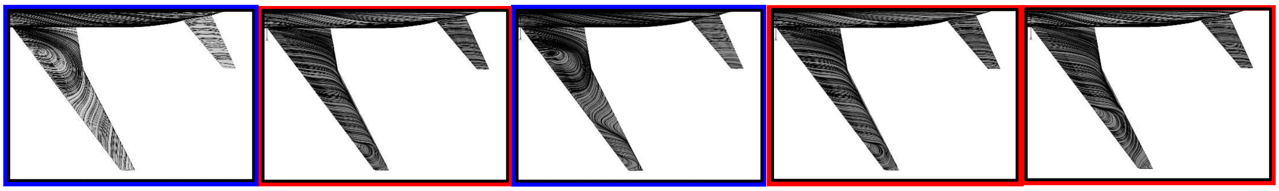

A1-BO-SST | A2-UP-SA | A3-UP-SST | A4-ME-SA | A5-ME-SST

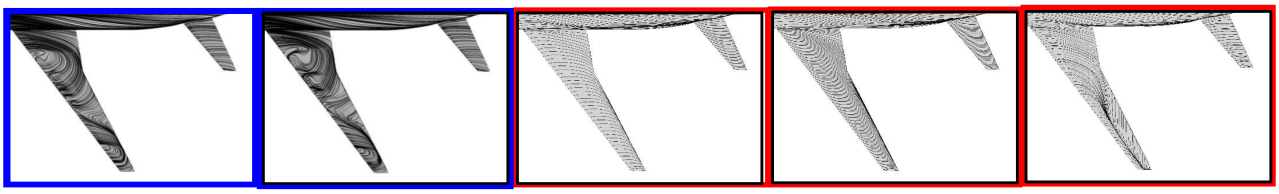

B1-Cu-SA | B2-Cu-SA | C1-Cu-SA | C2-Cu-SA | D1-Cu-SA

17

Surface streamline(13.08deg)

The flow tends to attach for Cartesian grid.
A4 and B1 are close to the experiment.

T. Uchiyama, et al., AIAA 2019-2190

CL-Alpha

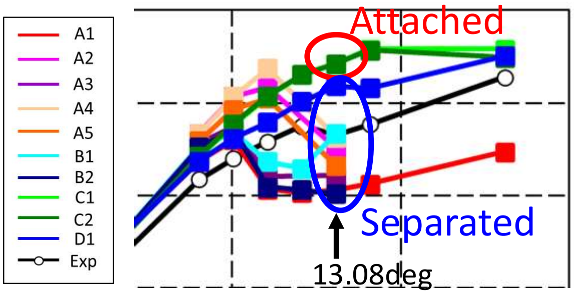

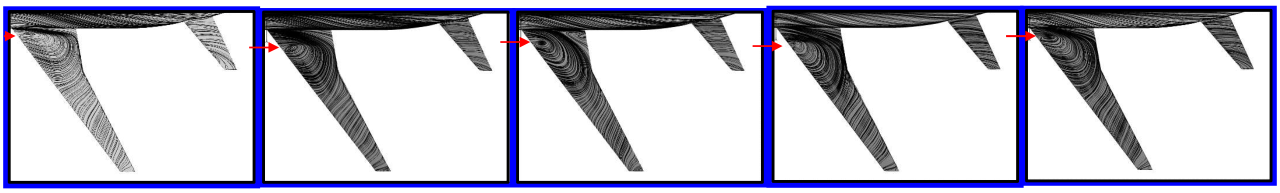

A1-BO-SST | A2-UP-SA | A3-UP-SST | A4-ME-SA | A5-ME-SST

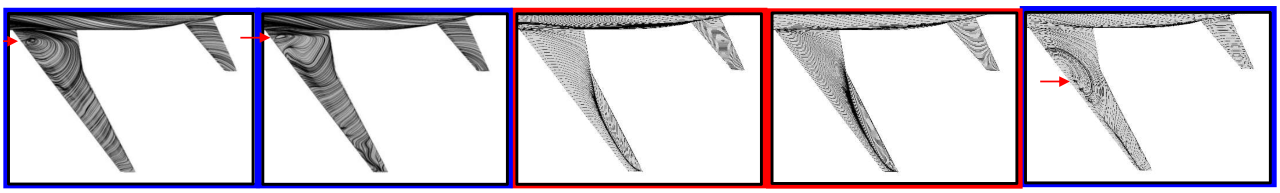

B1-Cu-SA | B2-Cu-SA | C1-Cu-SA | C2-Cu-SA | D1-Cu-SA

18

Wake interference with tail (11.05deg, Section YB)

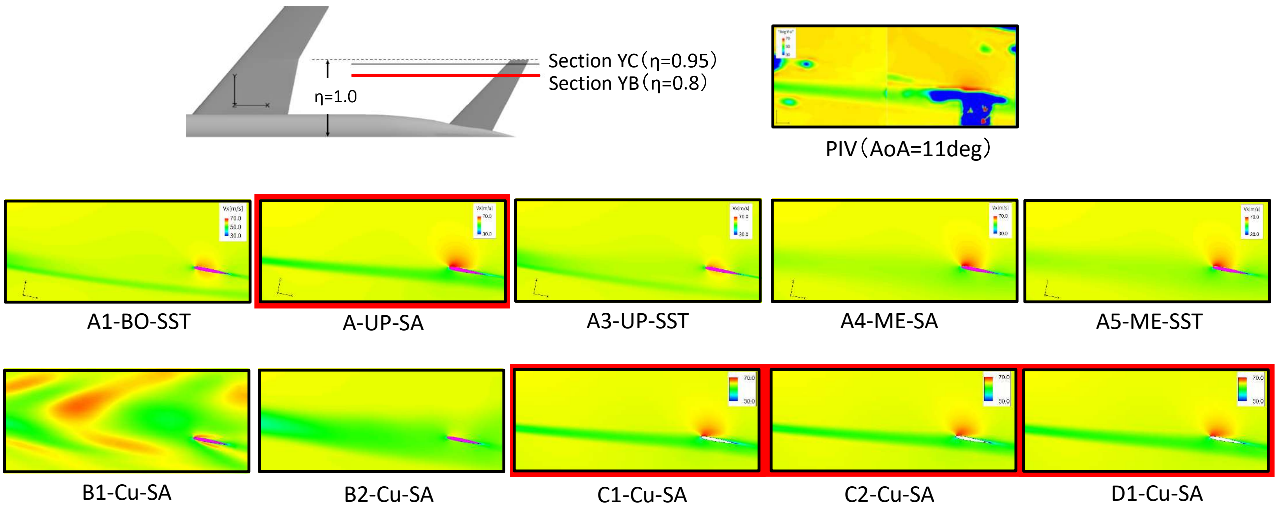

The attached cases are close to the experiment

Wake interference with tail (11.05deg, Section YC)

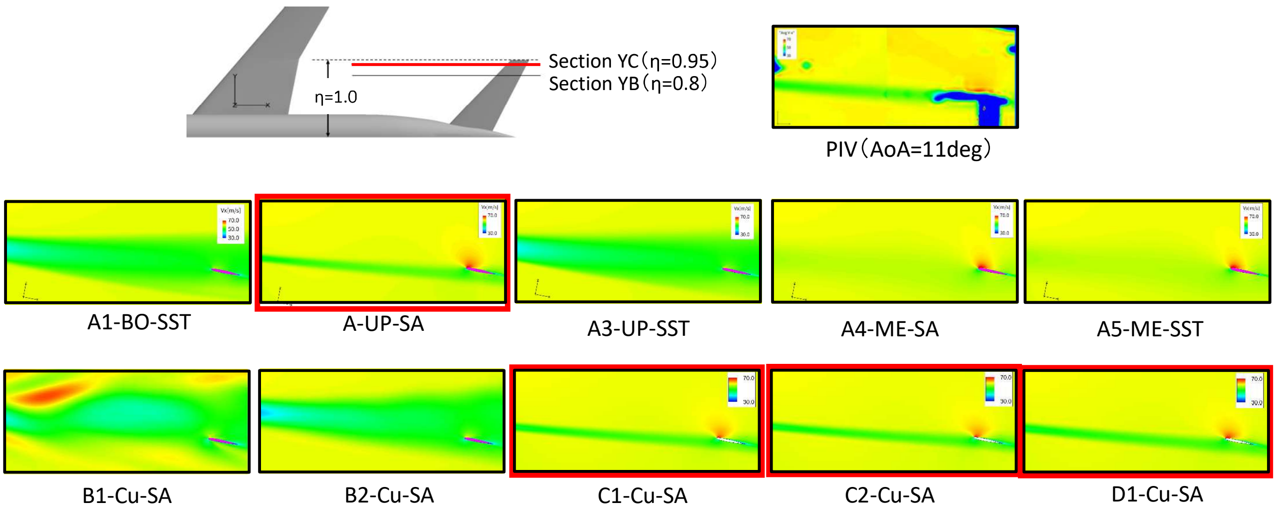

The attached cases are close to the experiment

Wake interference with tail (13.08deg, Section YB)

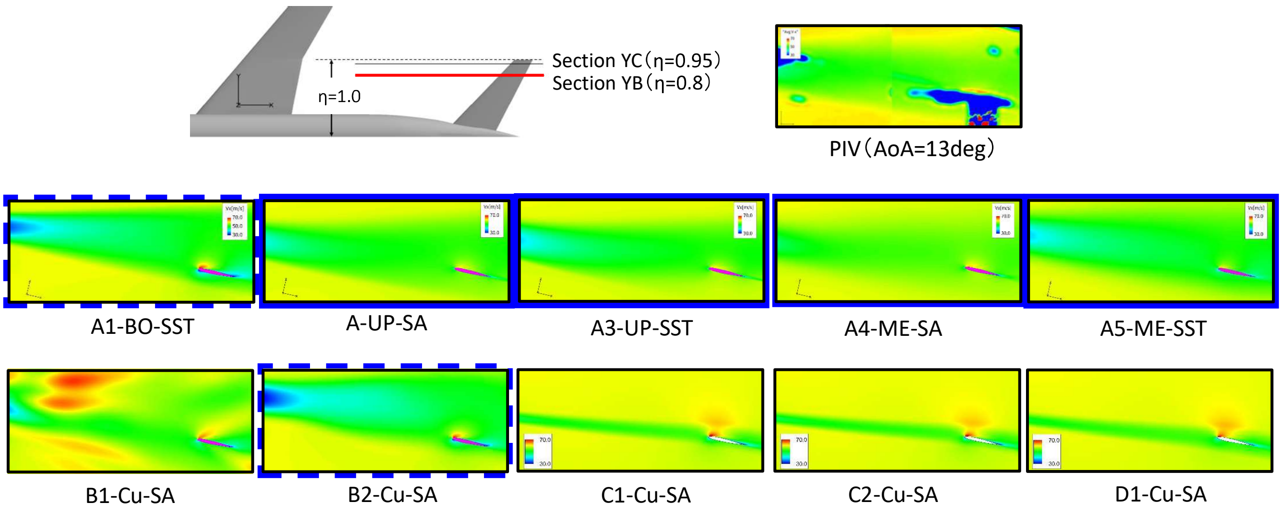

The separated cases are close to the experiment

Wake interference with tail (13.08deg, Section YC)

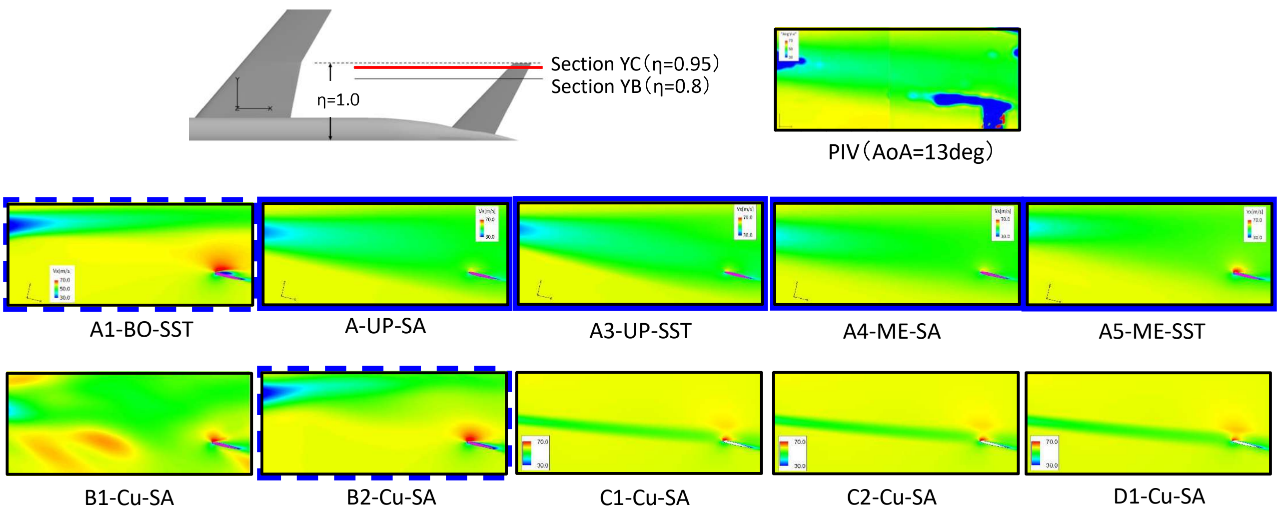

The separated cases are close to the experiment

Velocity contours (11.05deg, Section XA)

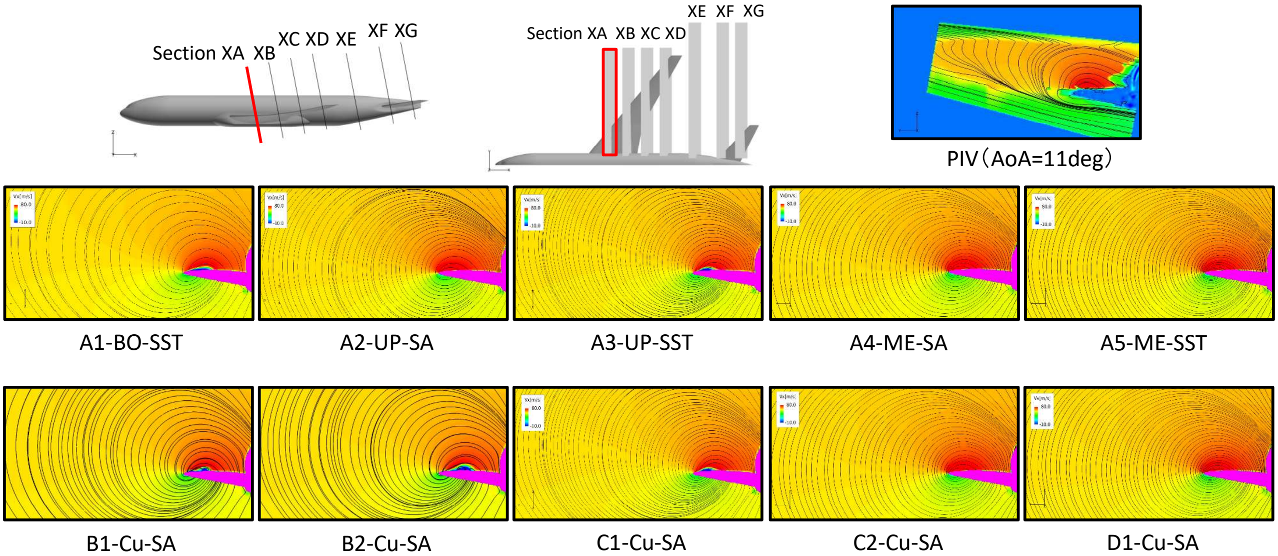

23

Velocity contours (11.05deg, Section XB)

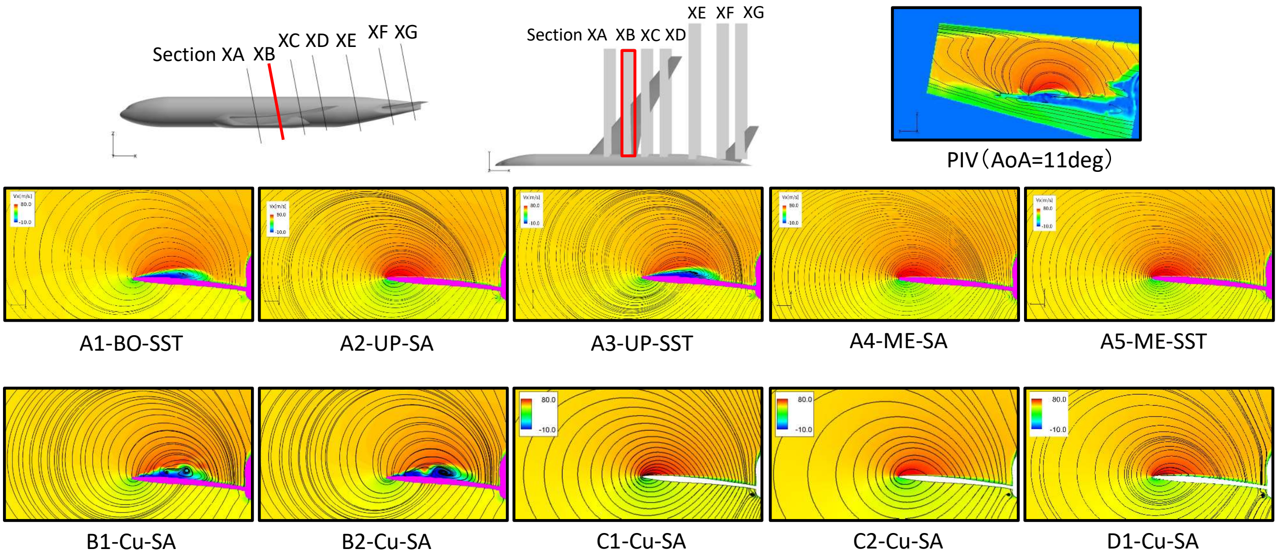

24

Velocity contours (11.05deg, Section XC)

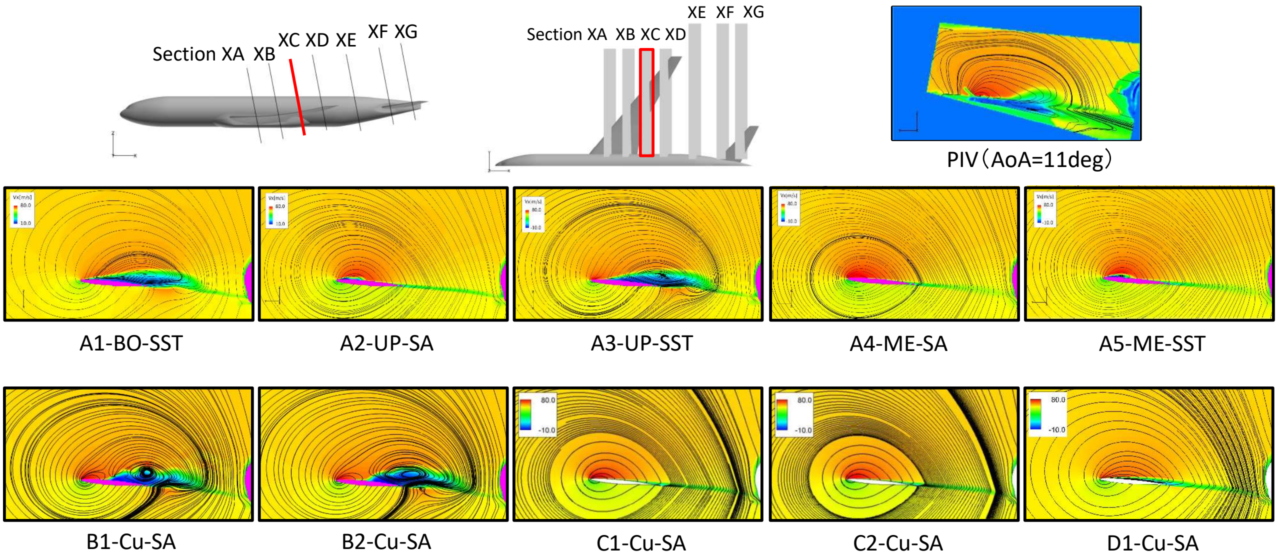

25

Velocity contours (11.05deg, Section XD)

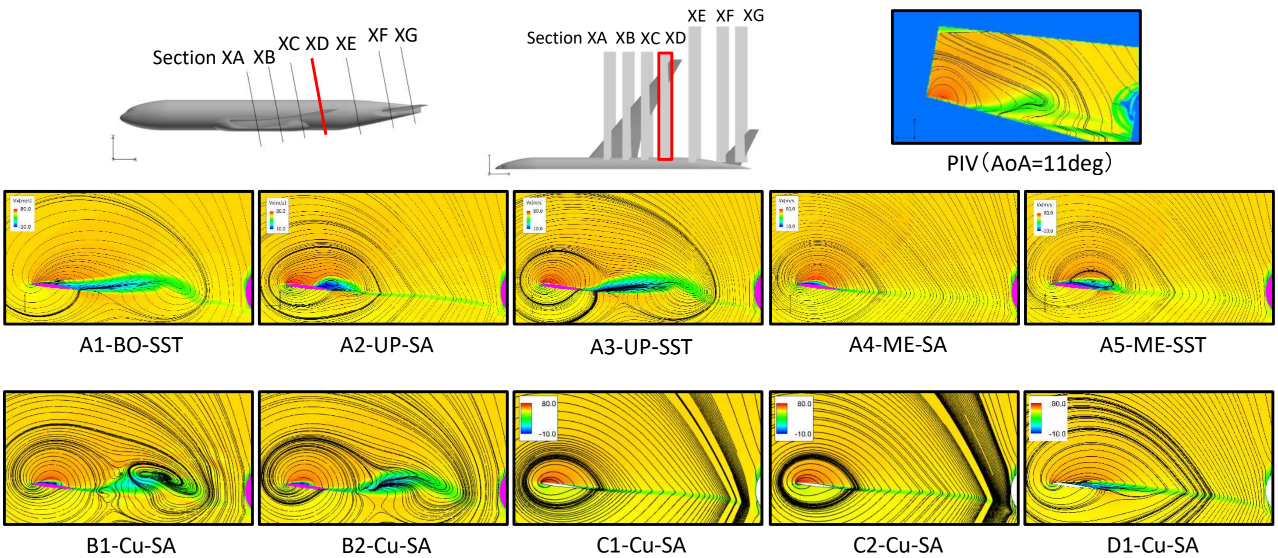

26

Velocity contours (11.05deg, Section XE)

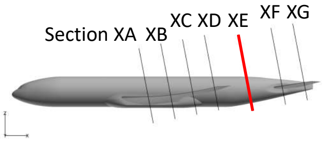

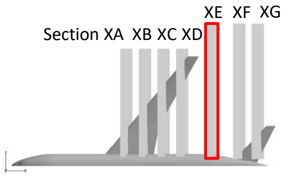

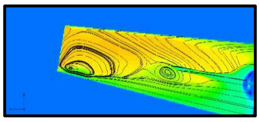

PIV（AoA=11deg）

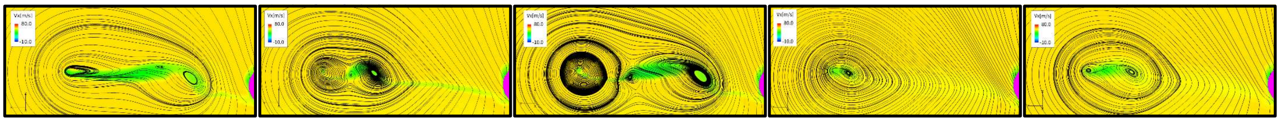

A1-BO-SST A2-UP-SA A3-UP-SST A4-ME-SA A5-ME-SST

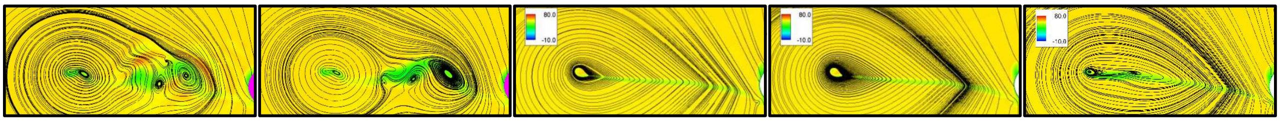

B1-Cu-SA B2-Cu-SA C1-Cu-SA C2-Cu-SA D1-Cu-SA

27

Velocity contours (11.05deg, Section XF)

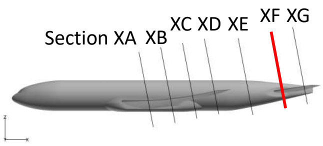

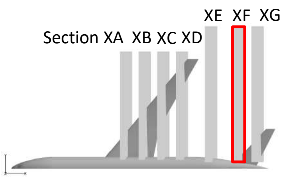

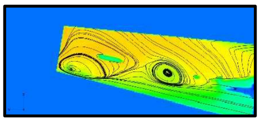

PIV（AoA=11deg）

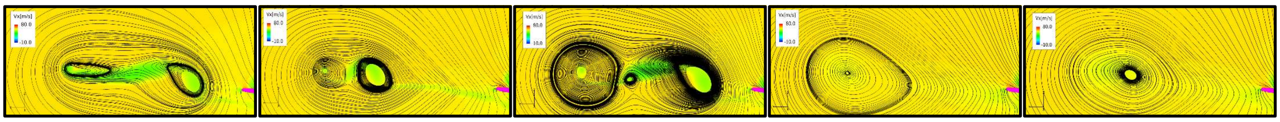

A1-BO-SST A2-UP-SA A3-UP-SST A4-ME-SA A5-ME-SST

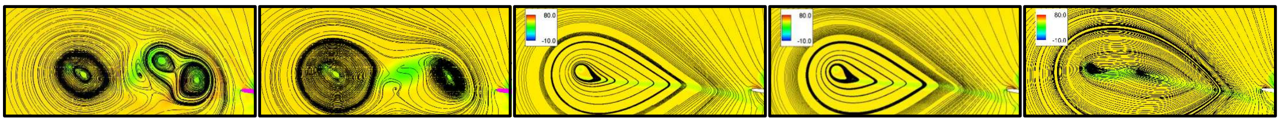

B1-Cu-SA B2-Cu-SA C1-Cu-SA C2-Cu-SA D1-Cu-SA

28

Velocity contours

(11.05deg, Section XG)

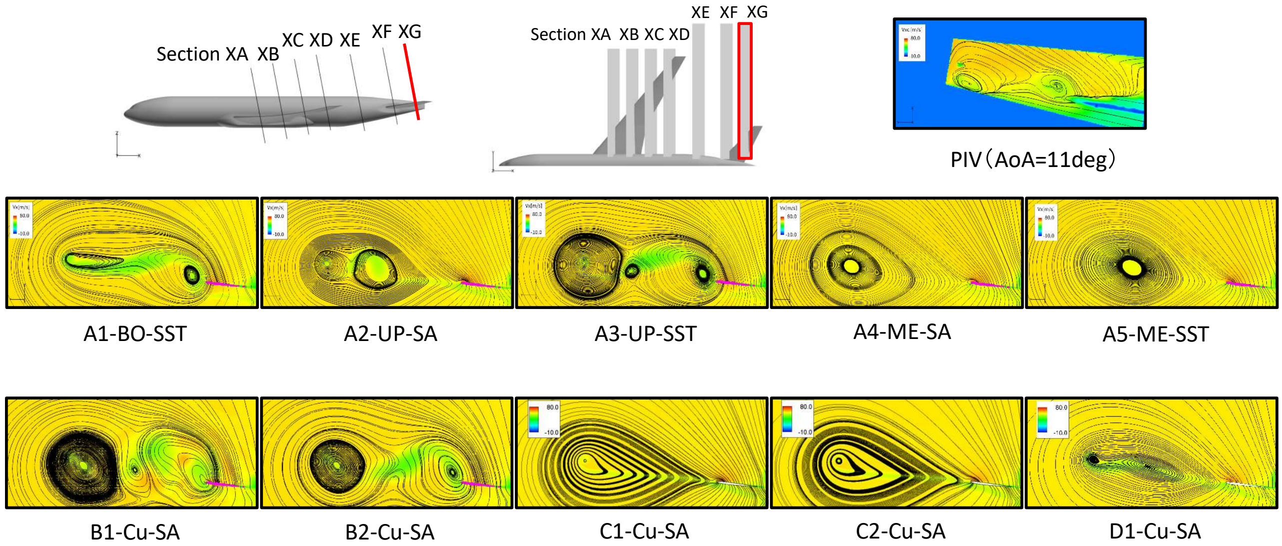

29

Velocity contours

(13.08deg, Section XA)

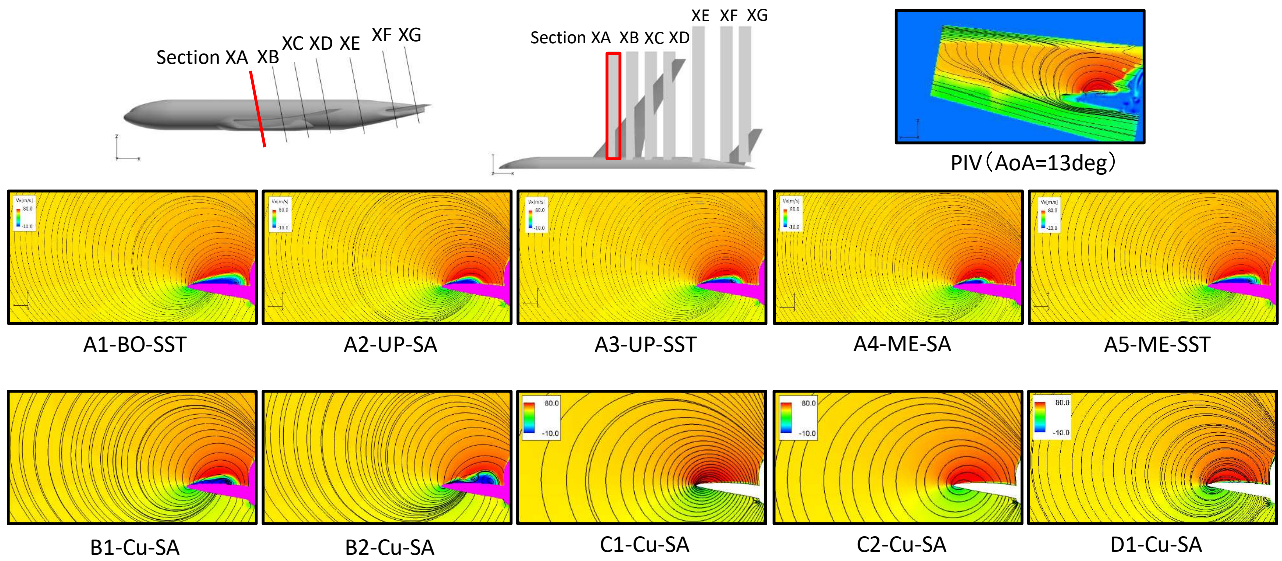

30

Velocity contours
(13.08deg, Section XB)

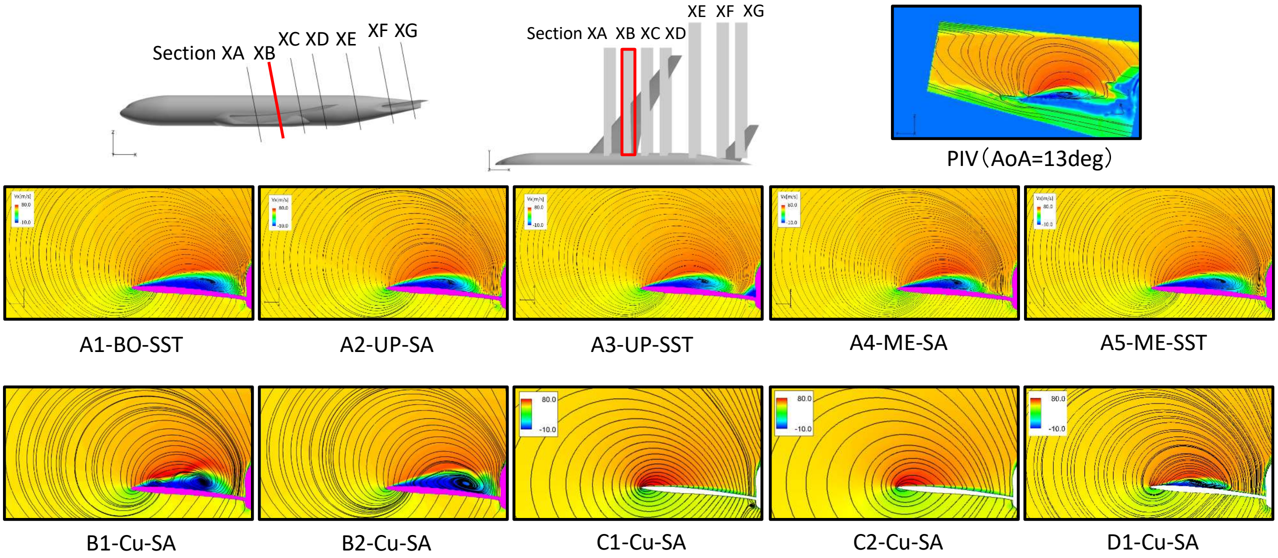

31

Velocity contours
(13.08deg, Section XC)

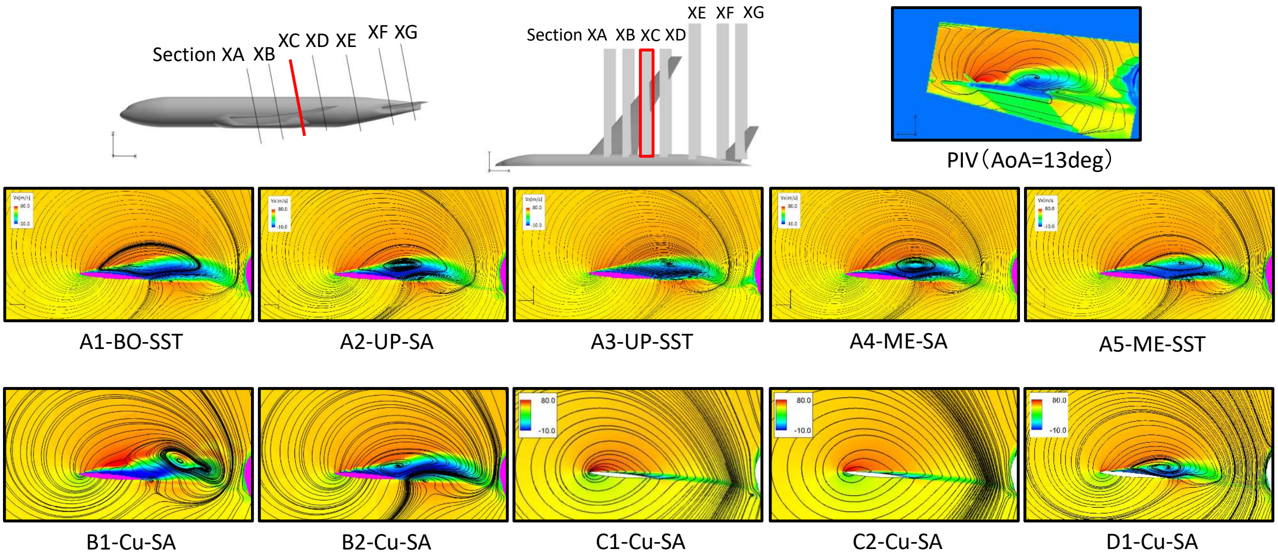

32

Velocity contours (13.08deg, Section XD)

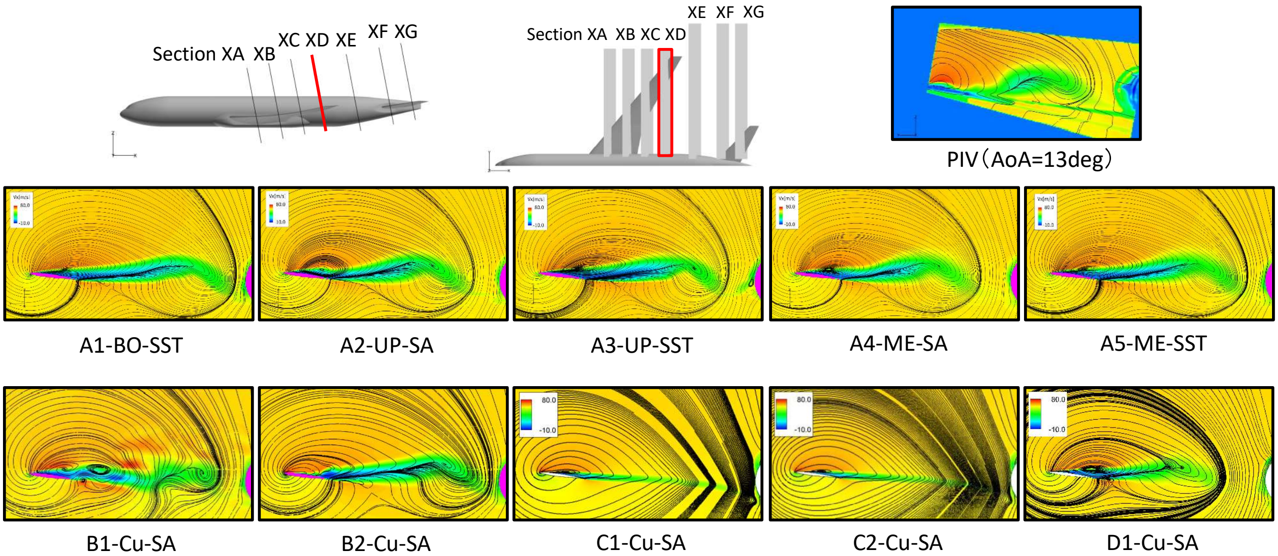

33

Velocity contours

(13.08deg, Section XE)

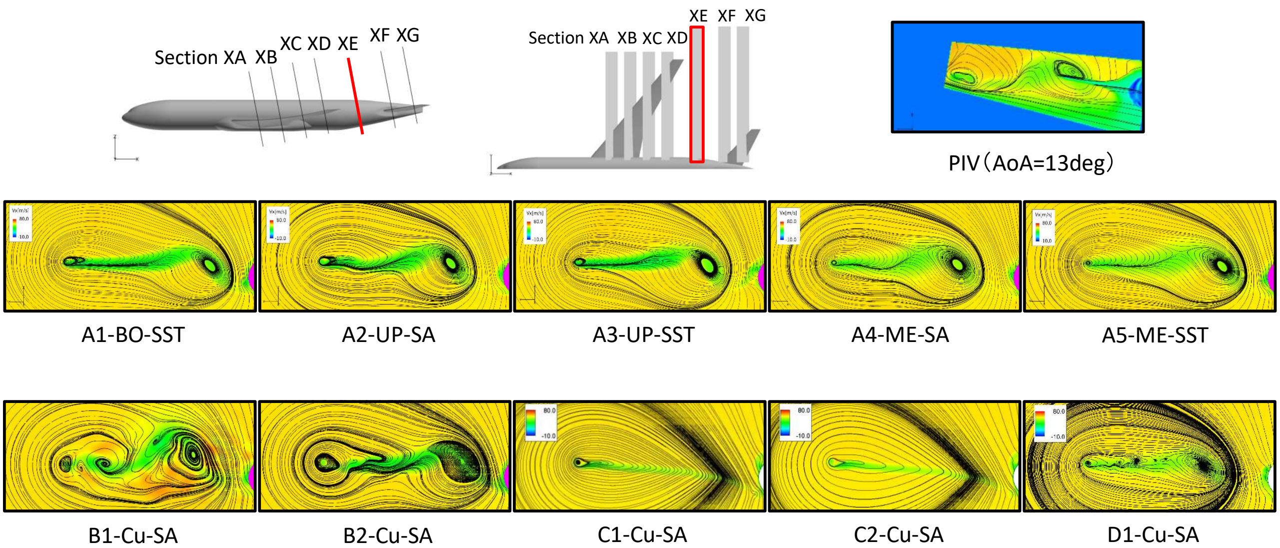

34

Velocity contours
(13.08deg, Section XF)

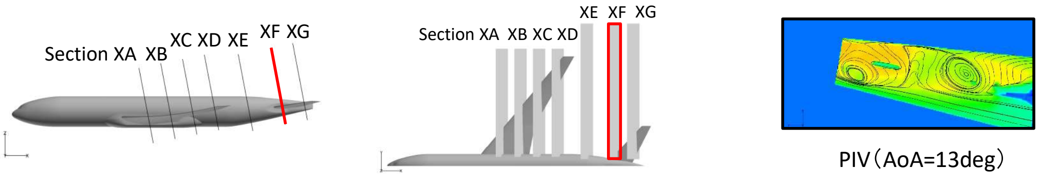

PIV（AoA=13deg）

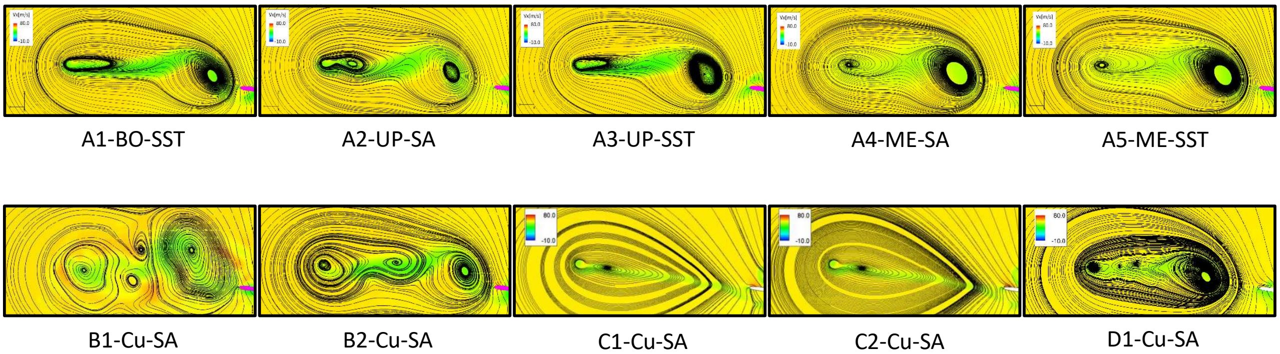

35

Velocity contours
(13.08deg, Section XG)

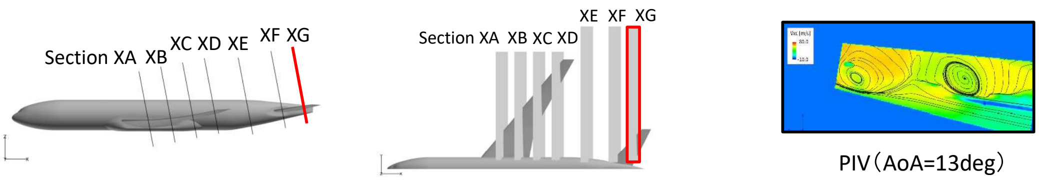

PIV（AoA=13deg）

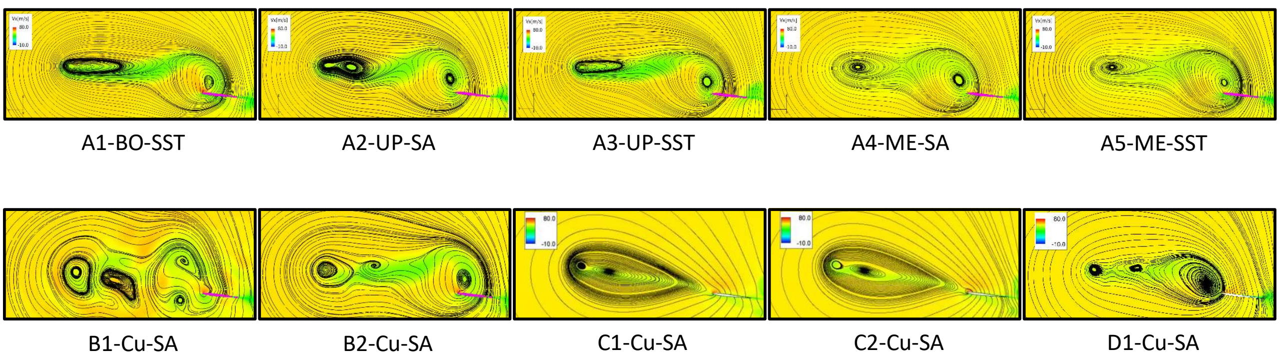

36

Surface Cp distribution（Tail, Section HB-HC）

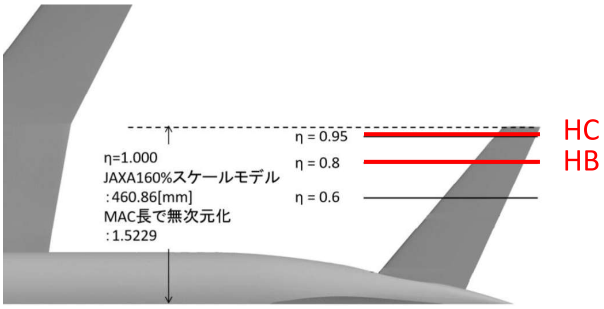

Cross section	η	y[mm]
Section HA	0.6	277
Section HB	0.8	369
Section HC	0.95	438

α[deg]	
CFD	EXP
-3.22	-3.0
-0.67	-0.5
2.89	3.0
5.95	6.0
9.01	9.0
10.03	10.0
11.05	11.0
12.06	12.1
13.08	13.0
14.08	14.1
18.08	18.1

37

Surface Cp distribution（Tail, Section HB-HC）

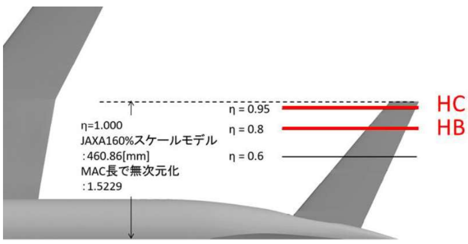

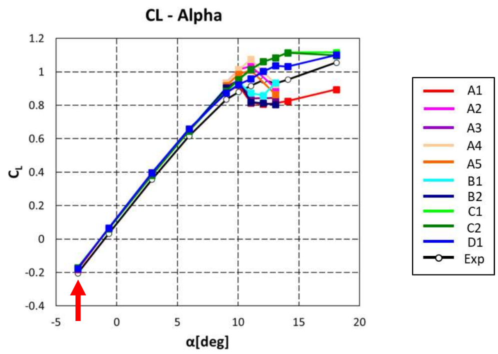

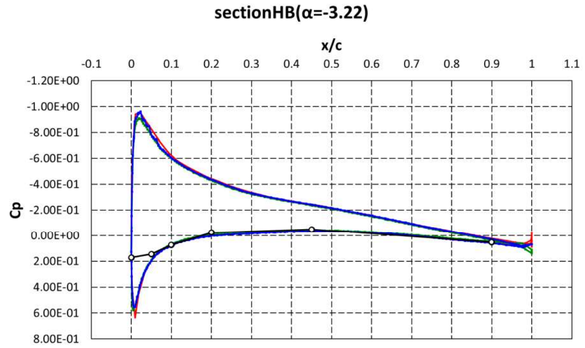

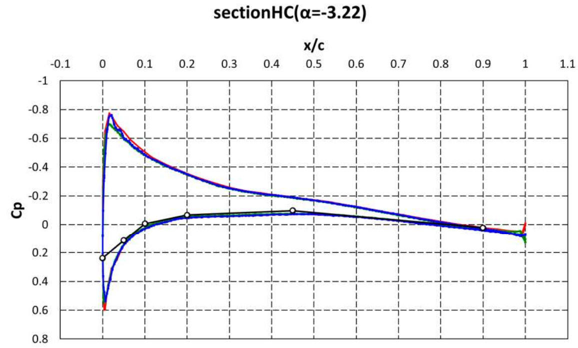

38

Surface Cp distribution（Tail, Section HB-HC）

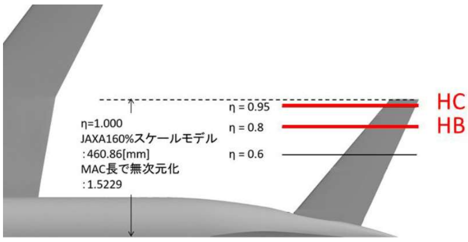

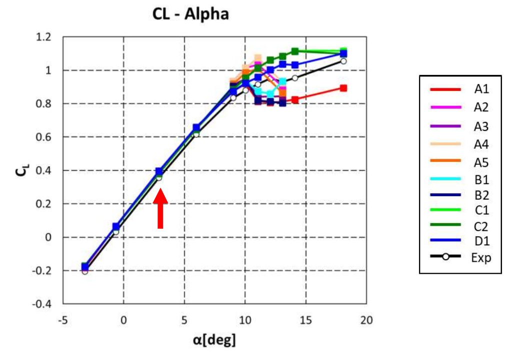

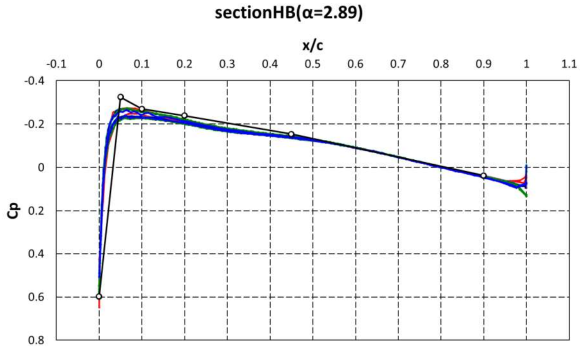

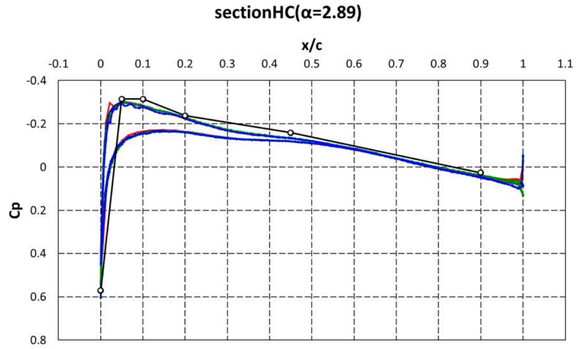

Surface Cp distribution（Tail, Section HB-HC）

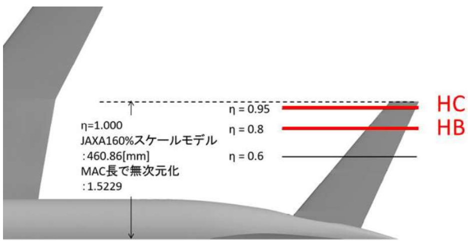

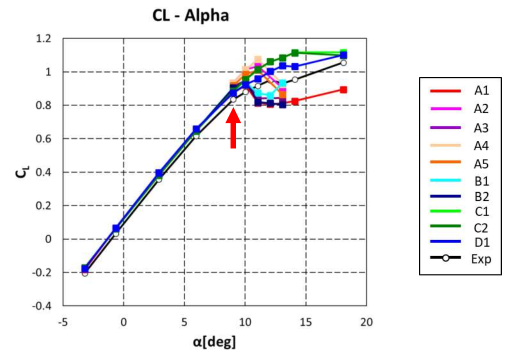

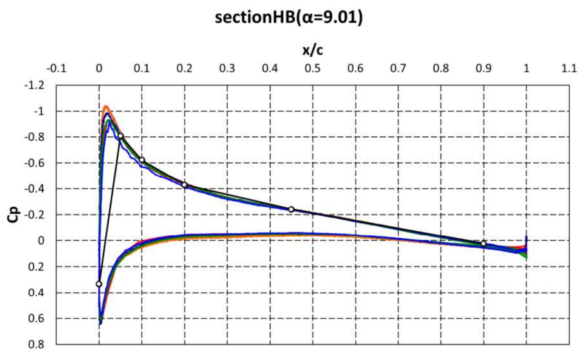

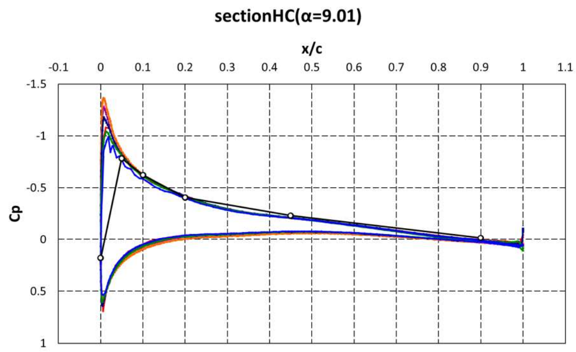

Surface Cp distribution（Tail, Section HB-HC）

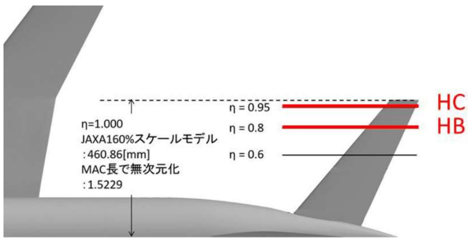

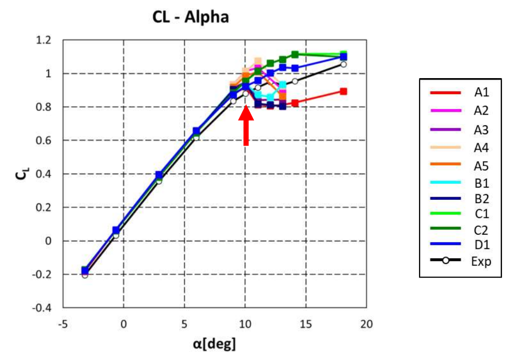

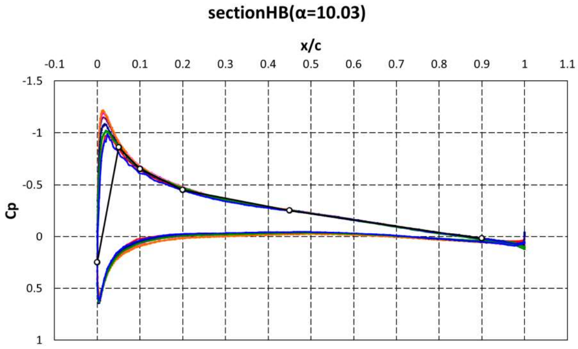

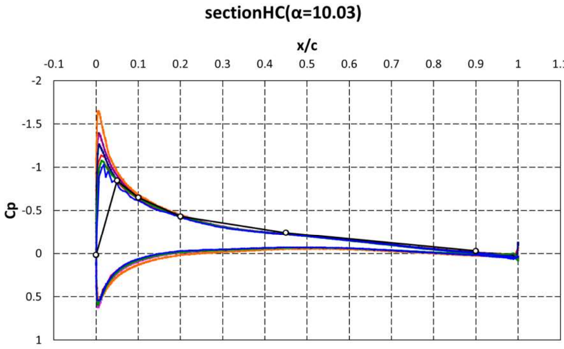

41

Surface Cp distribution（Tail, Section HB-HC）

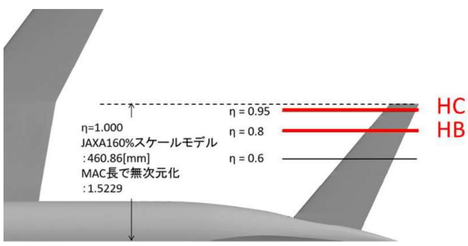

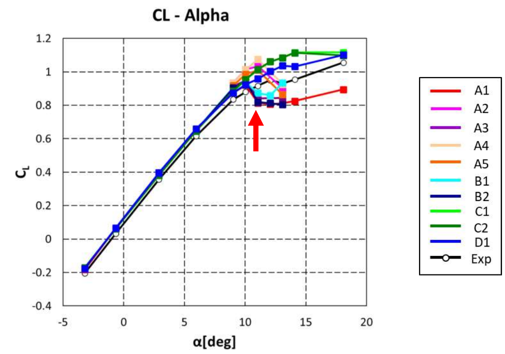

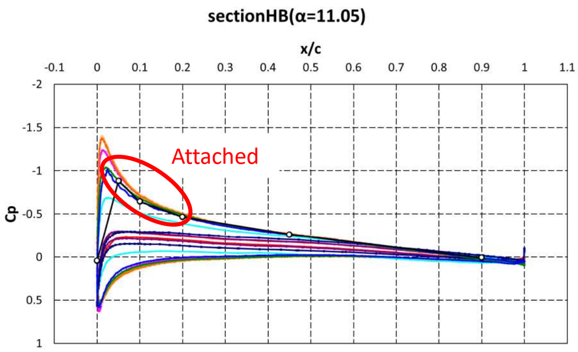

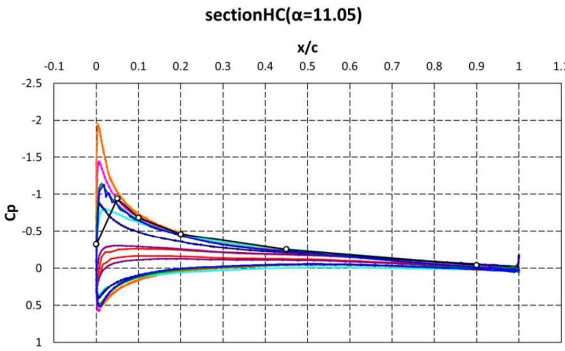

The attached cases are close to the experiment

42

Surface Cp distribution（Tail, Section HB-HC）

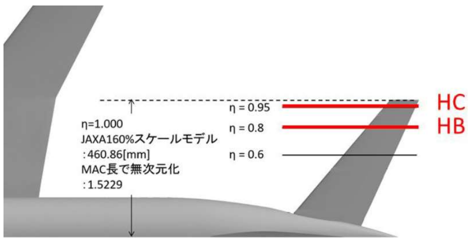

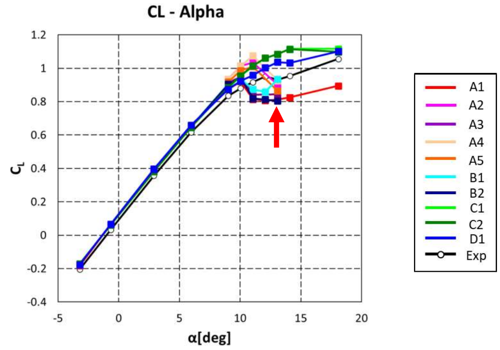

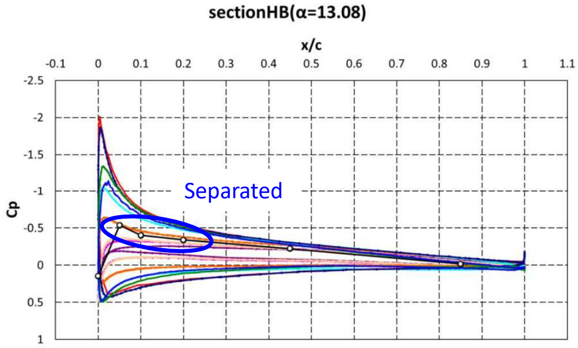

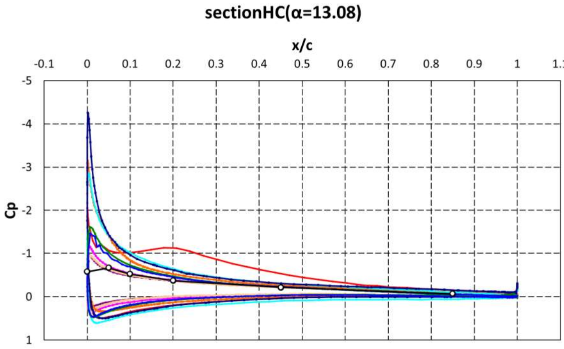

The separated cases are close to the experiment

43

Surface Cp distribution（Tail, Section HB-HC）

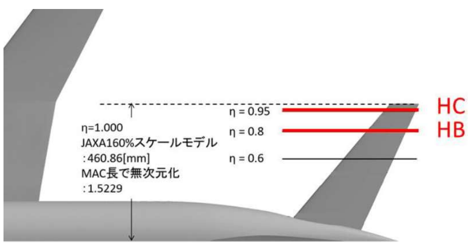

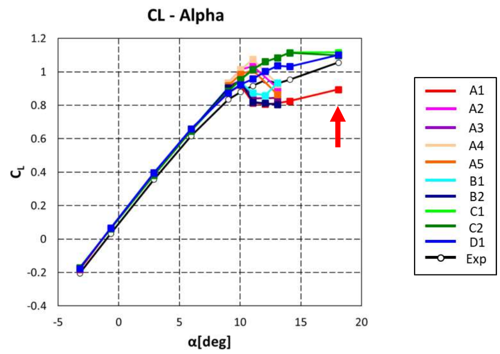

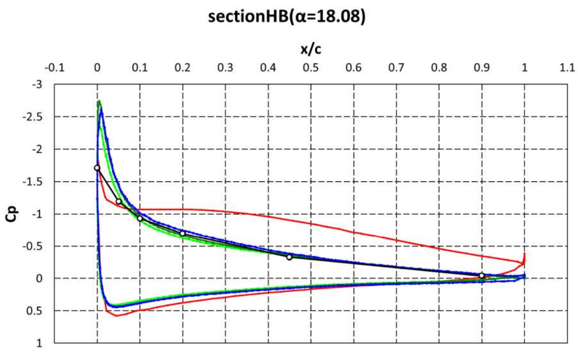

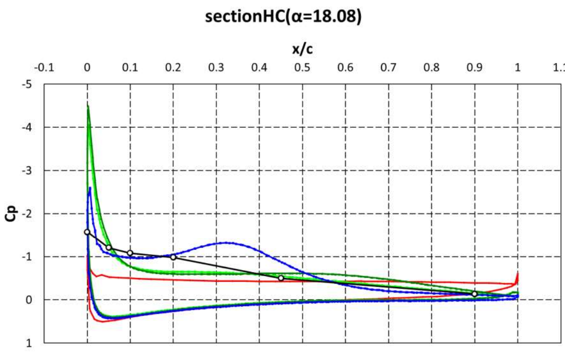

44

Case2 : Unsteady computation

- Aims
  - Understand the prediction accuracy of unsteady computation by comparing the unsteady computation with the steady computation.
  - Understand the dependency of turbulence model, grid, time step.
- Conditions
  - M = 0.168, $Re_c = 1.06 \times 10^6$, T_{ref}=310K
  - AoA = 11.05, 13.08deg

45

CL-Alpha, case2

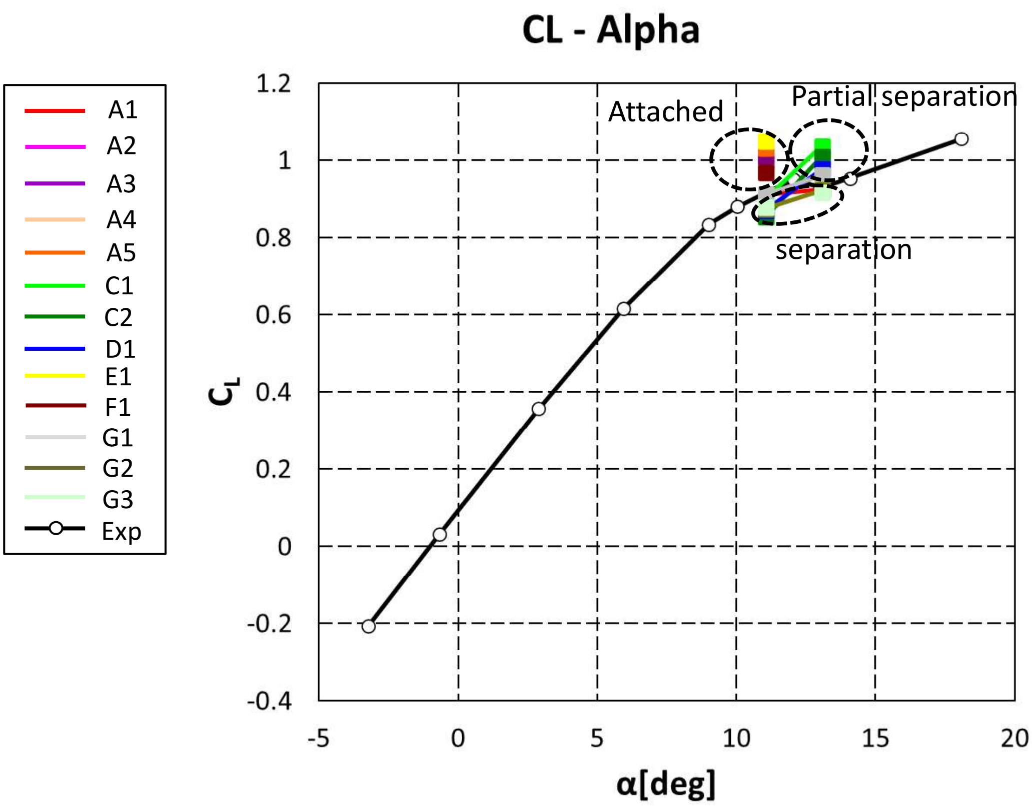

46

CD-Alpha, case2

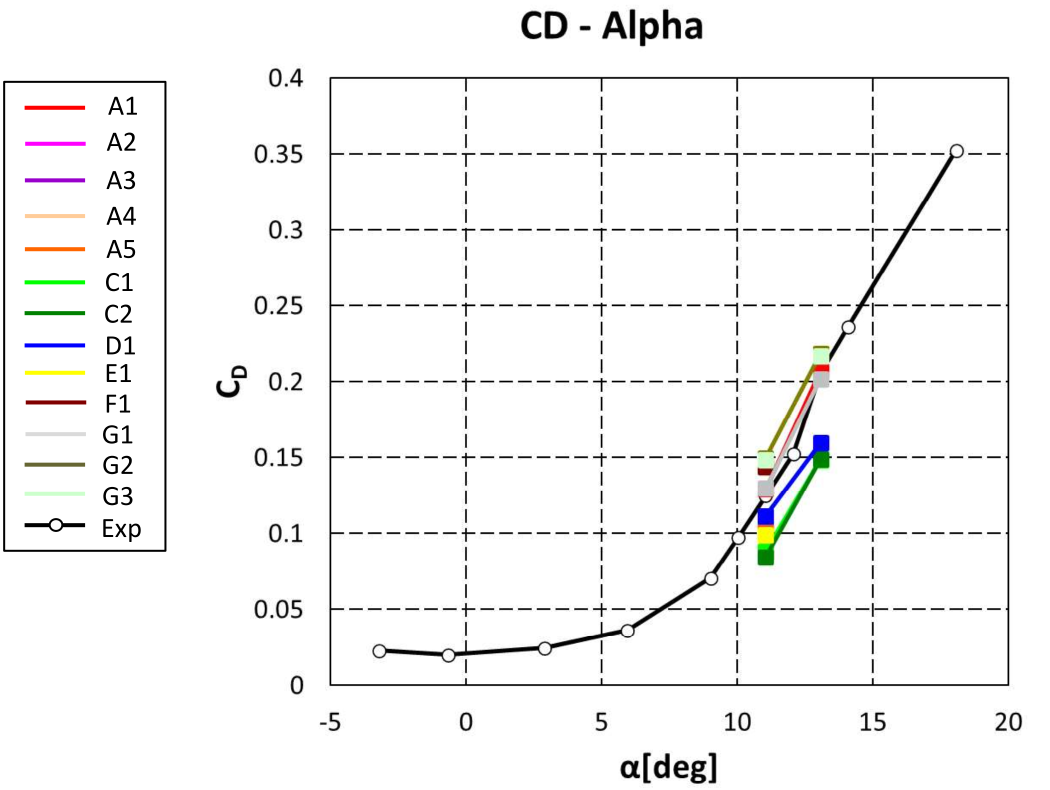

47

Cm-Alpha, case2

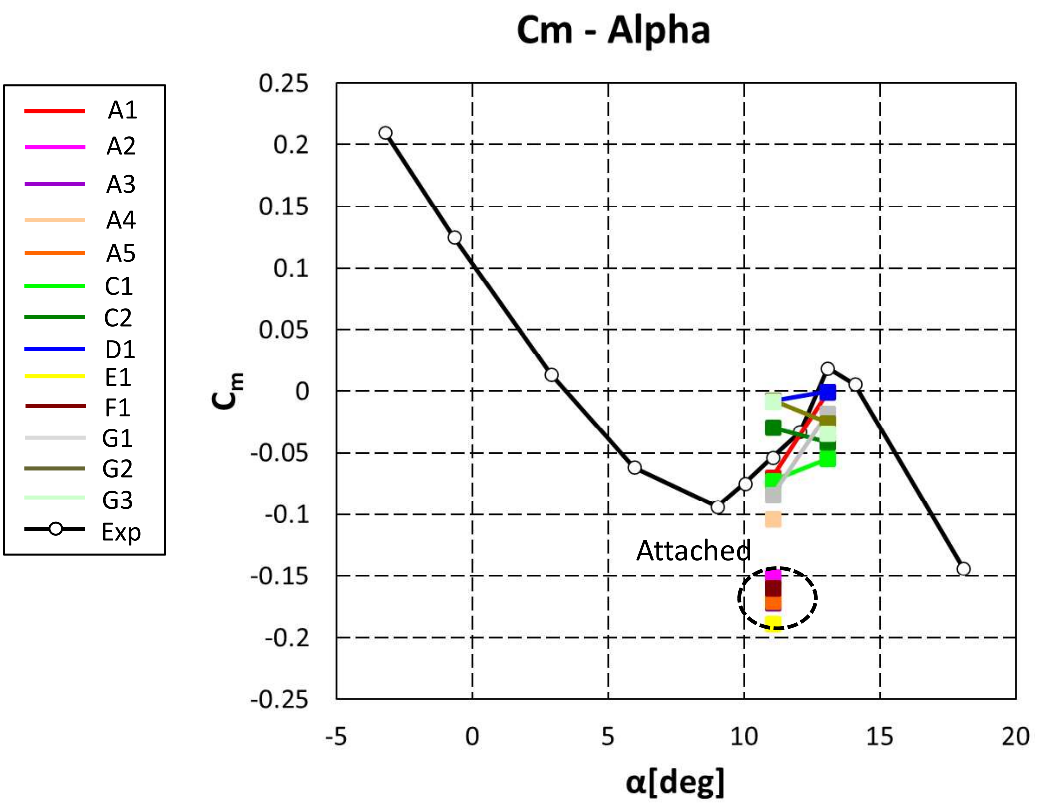

48

CL-Alpha

Steady (Case1)

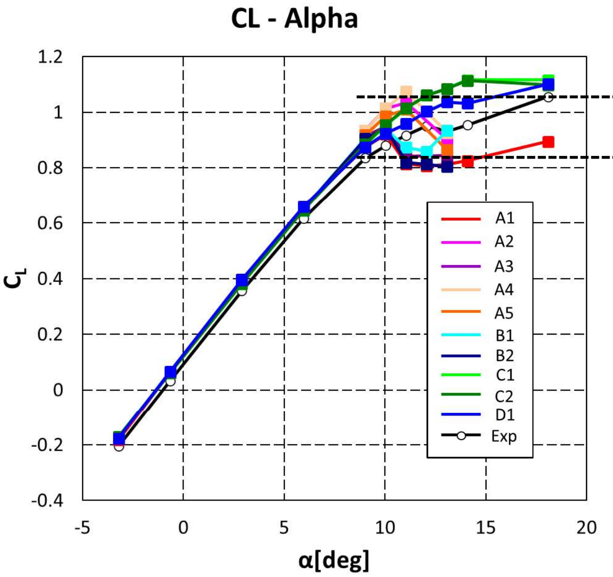

Unsteady (Case2)

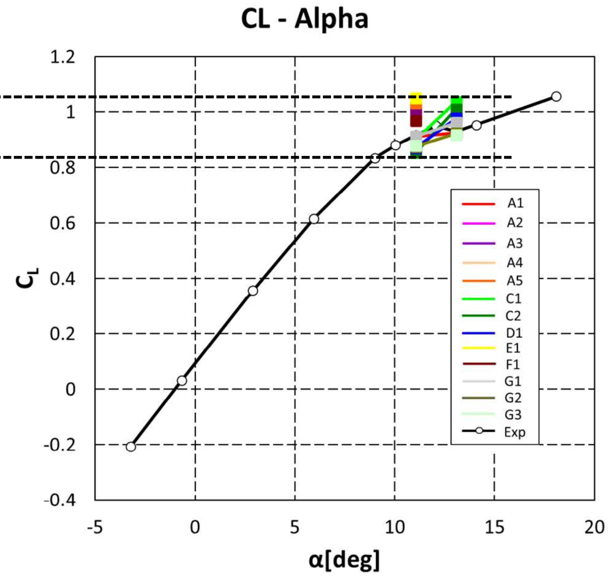

CL-Alpha

Steady (Case1)

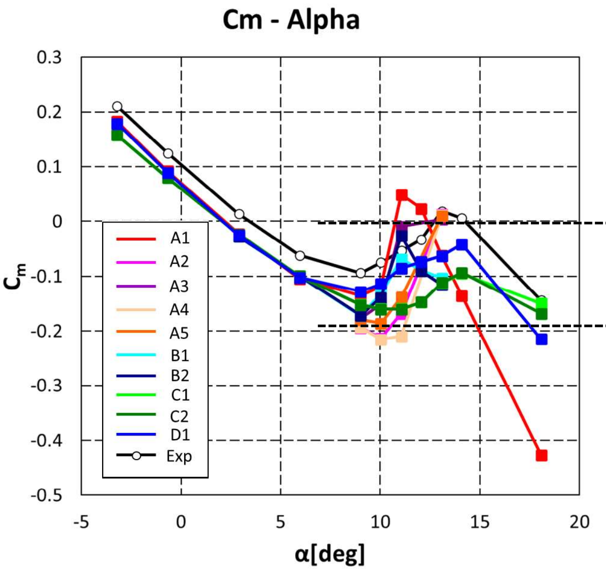

Unsteady (Case2)

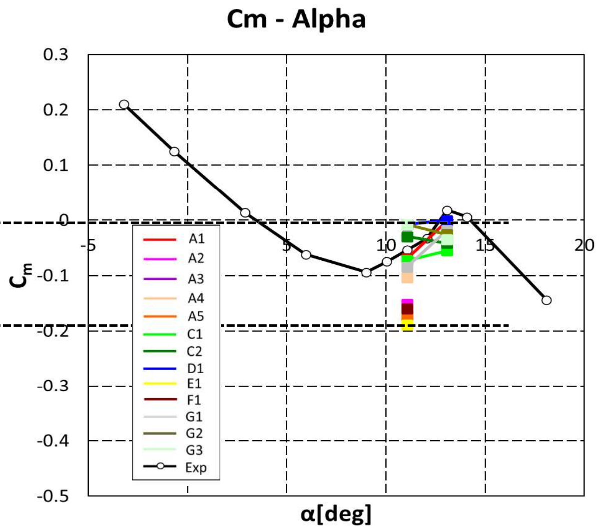

CL-Alpha

Steady (Case1)

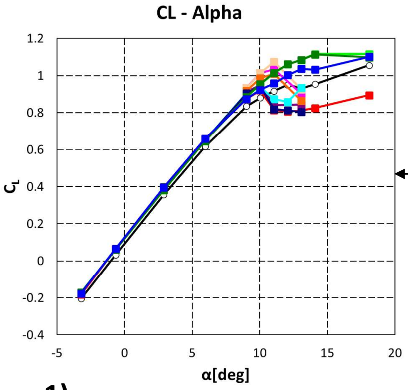

Unsteady (Case2)

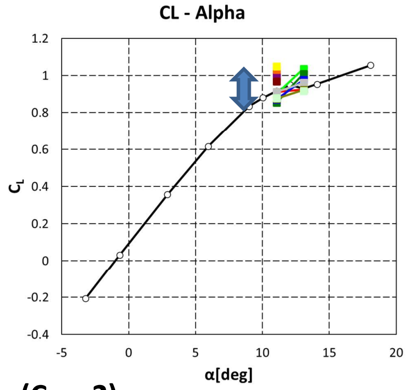

←APC-7→

Steady (Case1)

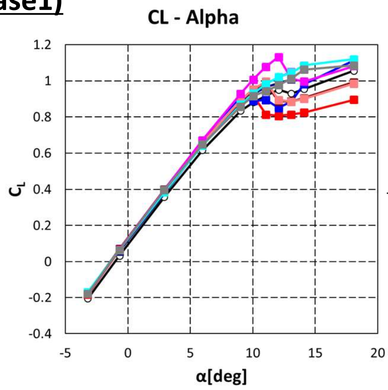

Unsteady (Case2)

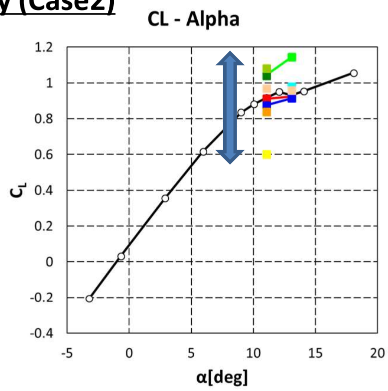

←APC-6→

Surface streamline(11.05deg, Average)

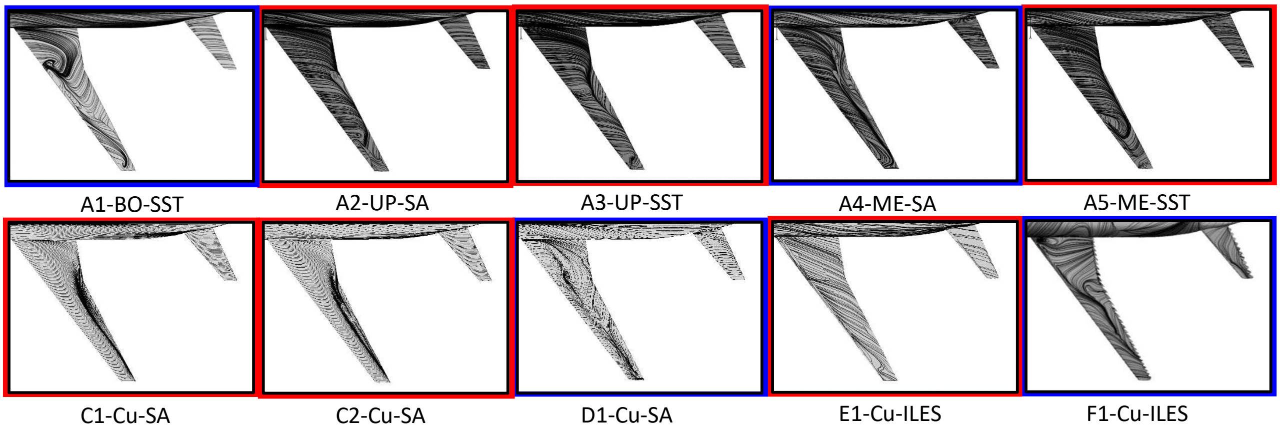

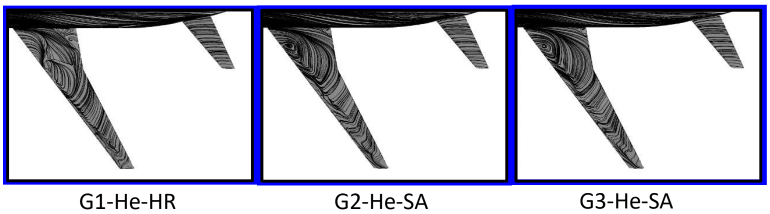

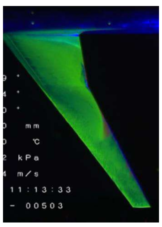

T. Uchiyama, et al., AIAA 2019-2190

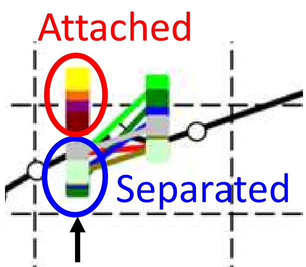

Surface streamline(13.08deg, Average)

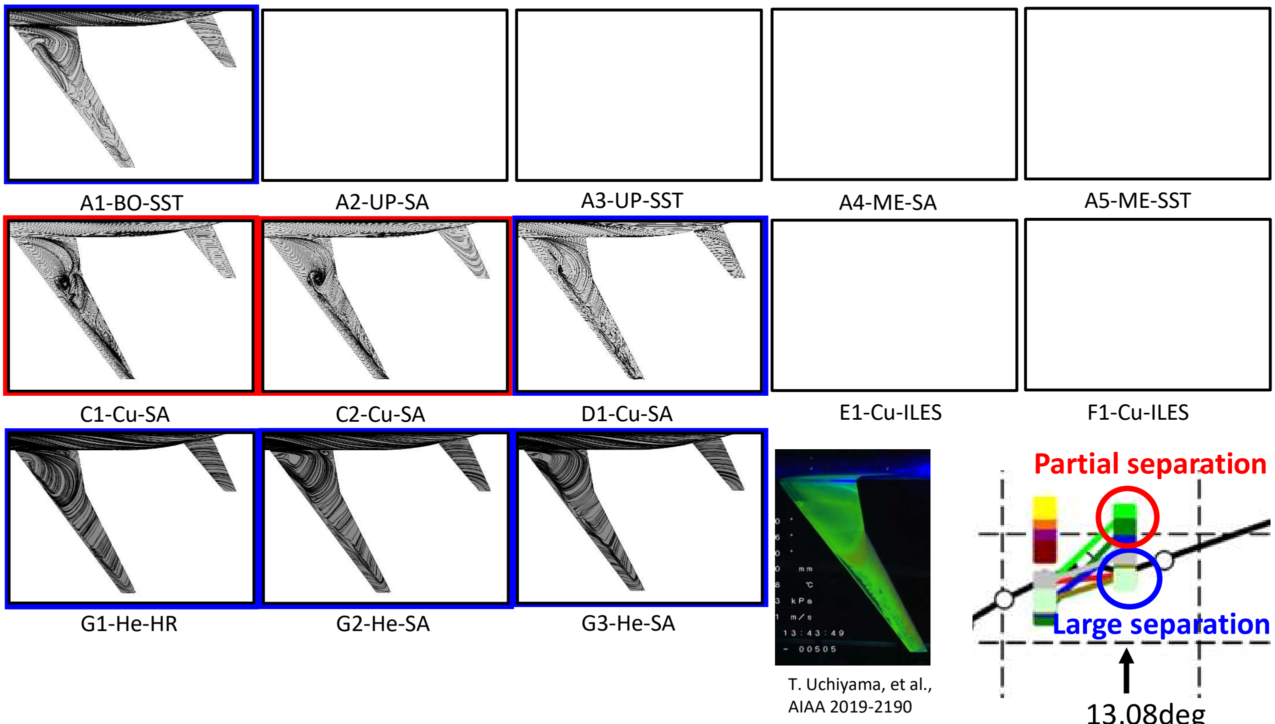

53

Wake interference with tail (11.05deg, Section YB, Average)

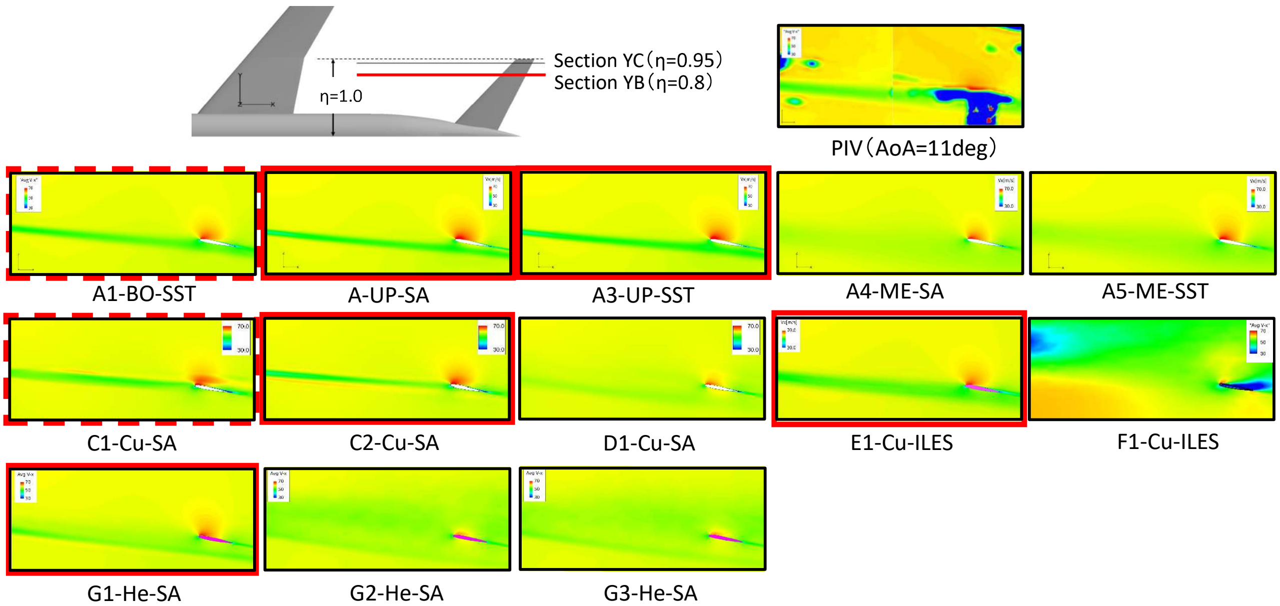

The attached cases are close to the experiment

54

Wake interference with tail (11.05deg, Section YC, Average)

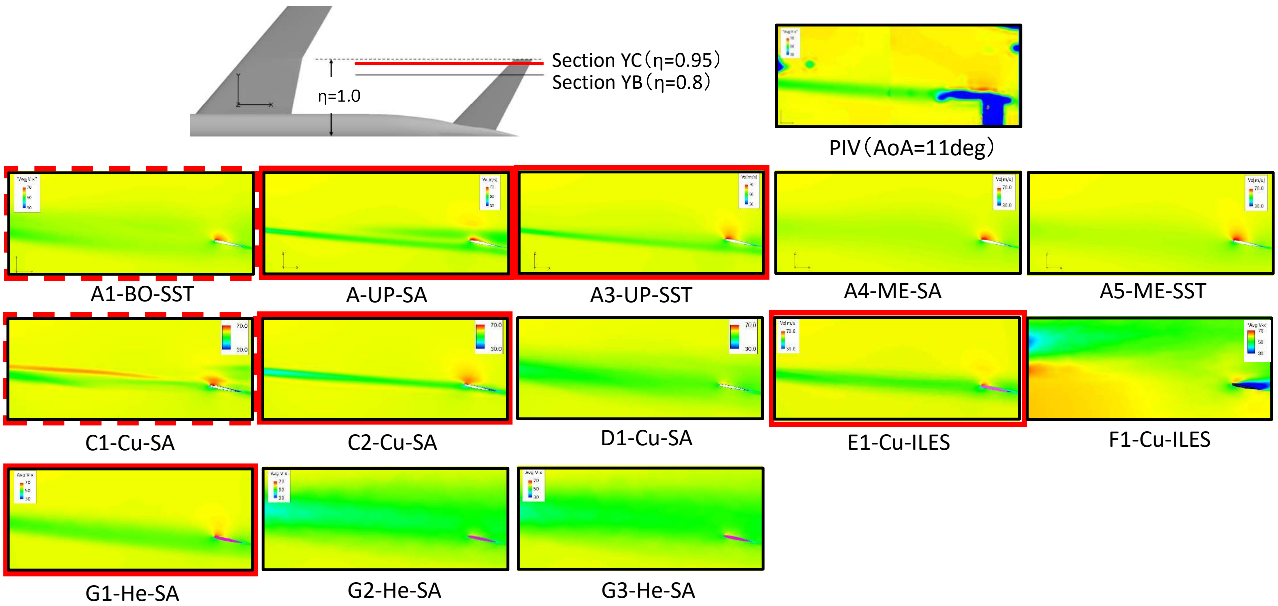

55

Wake interference with tail (13.08deg, Section YB, Average)

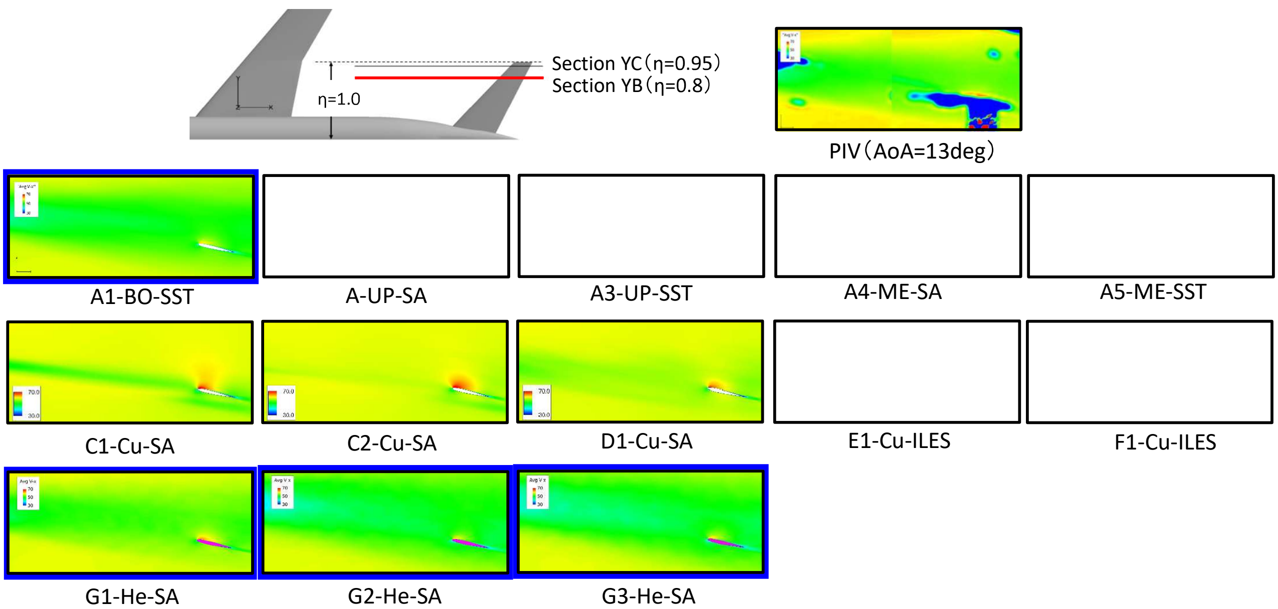

The separated cases are close to the experiment

56

Wake interference with tail (13.08deg, Section YC, Average)

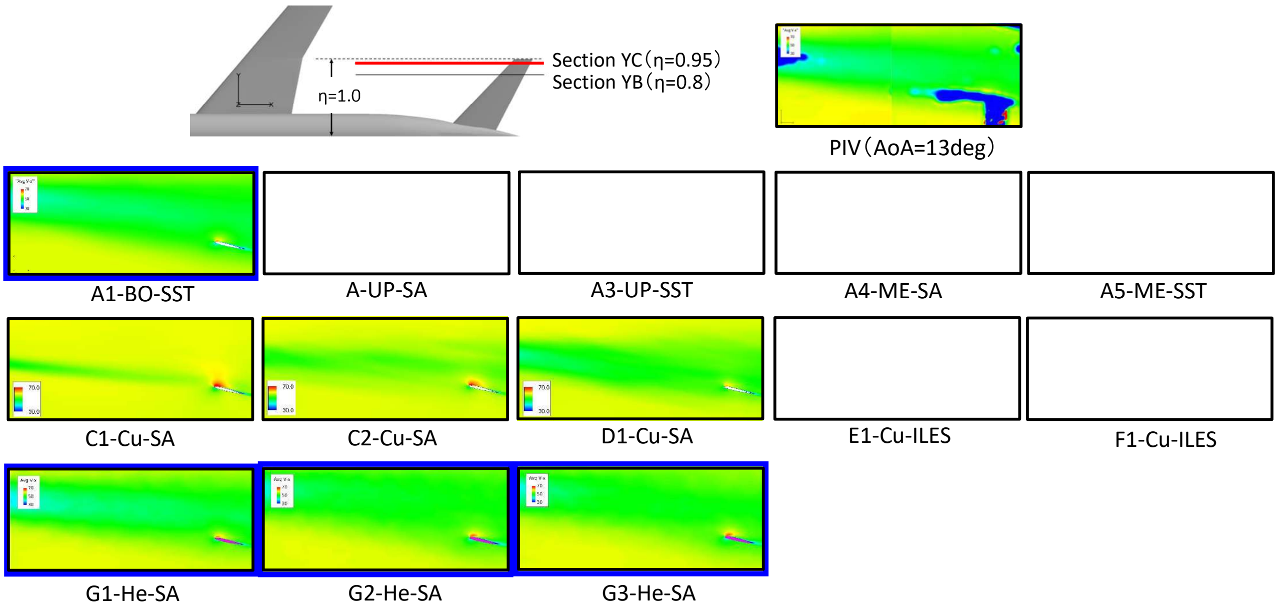

The separated cases are close to the experiment

57

Velocity contours (11.05deg, Section XA)

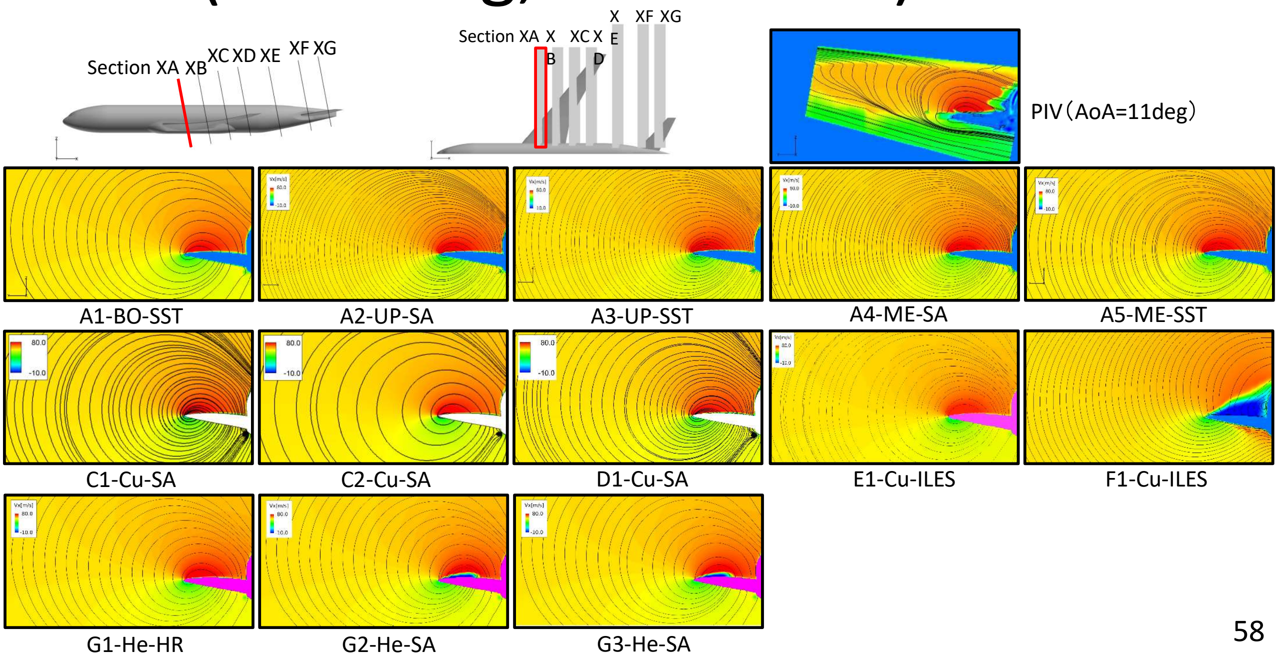

58

Velocity contours (11.05deg, Section XB)

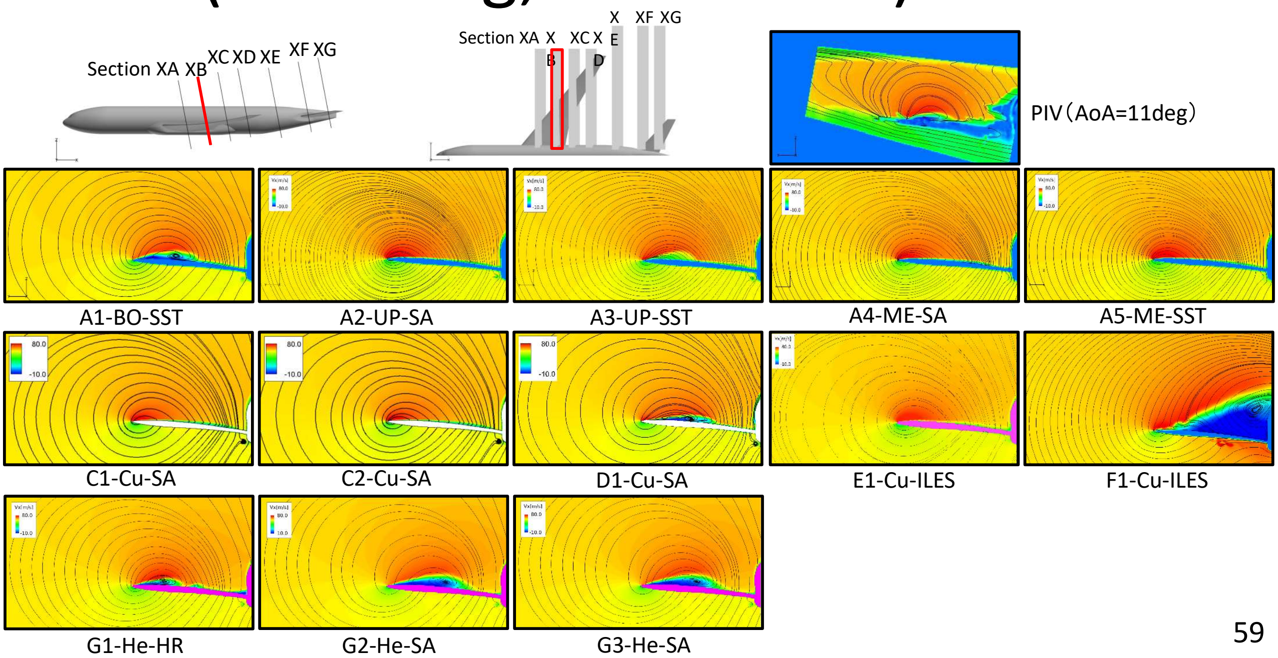

59

Velocity contours (11.05deg, Section XC)

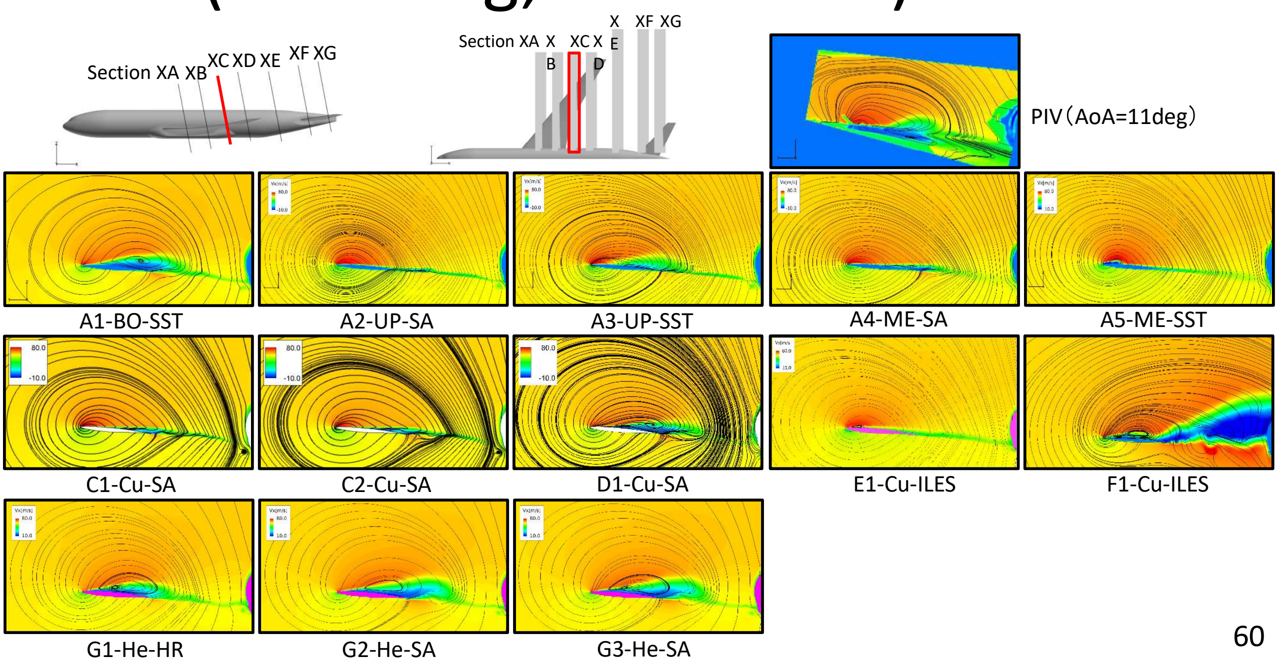

60

Velocity contours (11.05deg, Section XD)

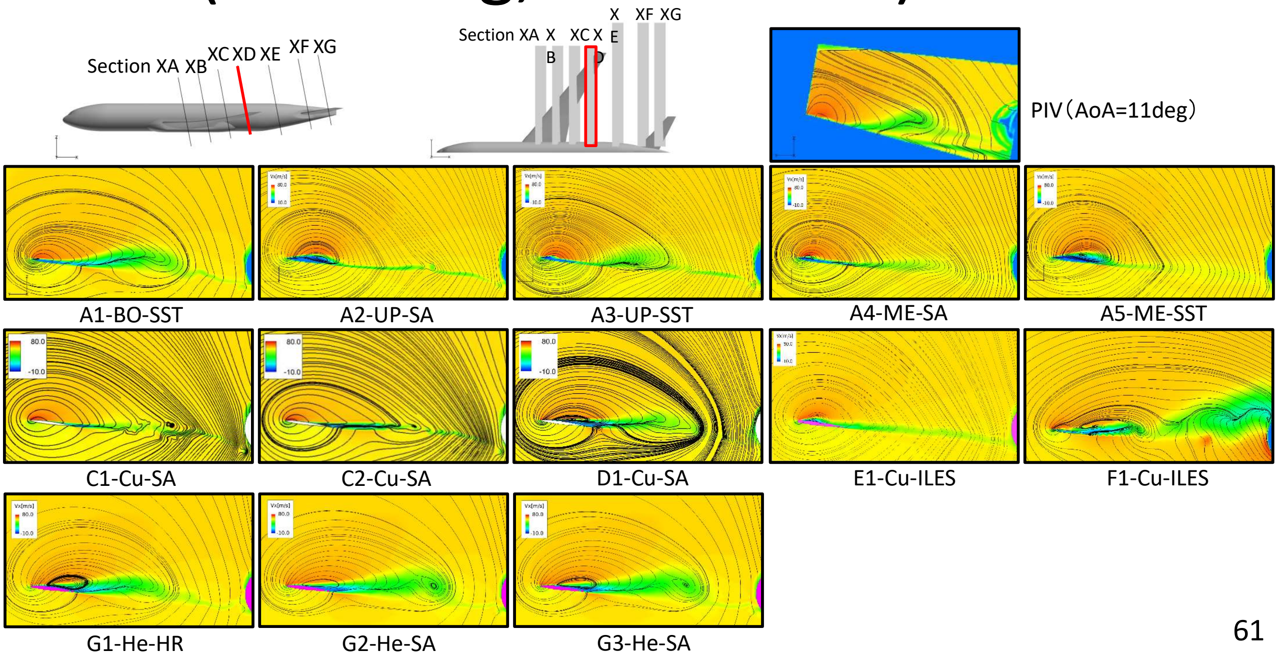

61

Velocity contours (11.05deg, Section XE)

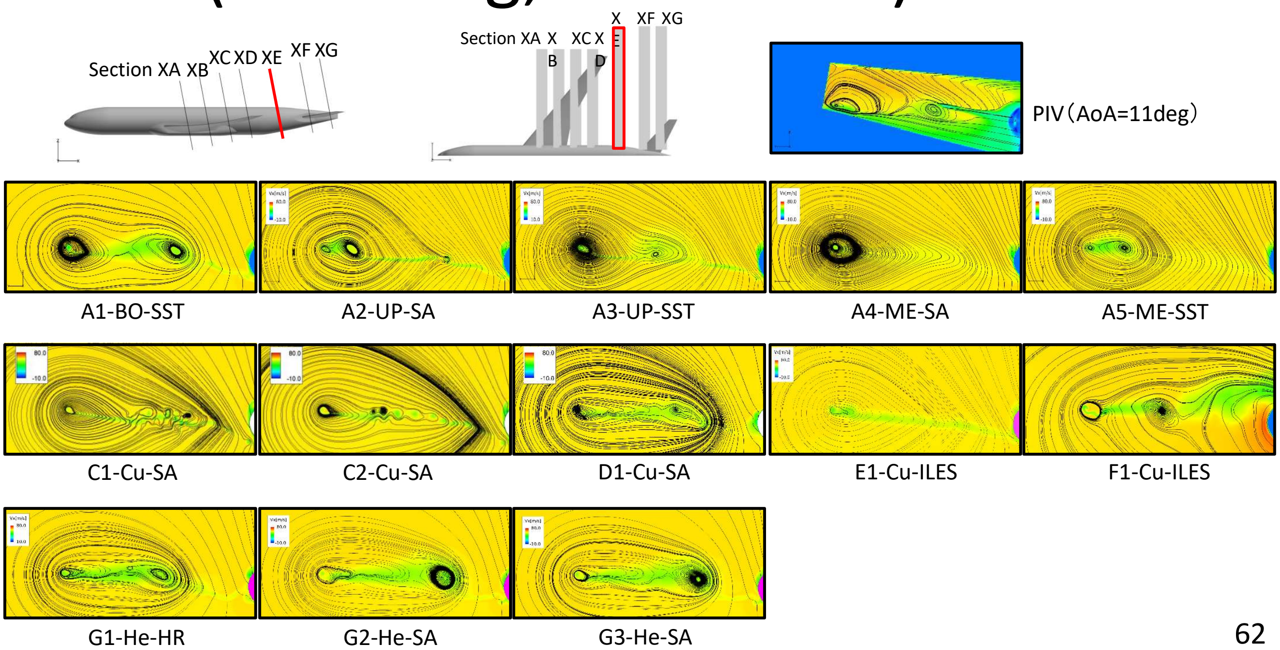

62

Velocity contours (11.05deg, Section XF)

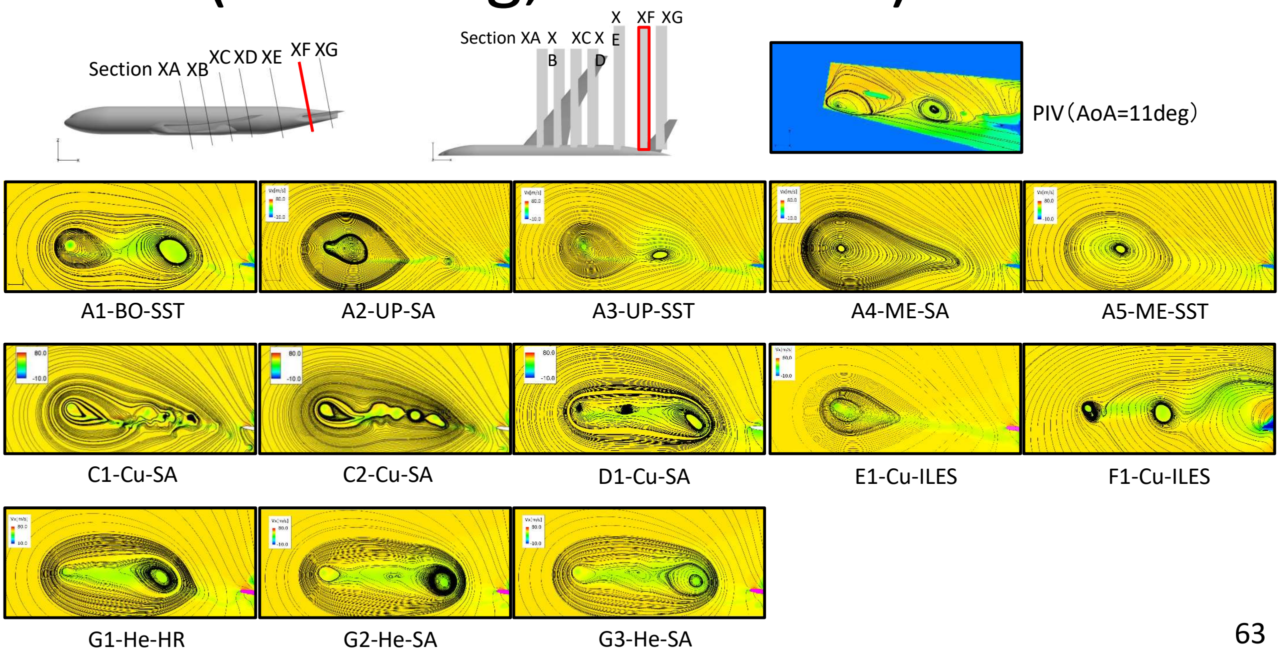

63

Velocity contours (11.05deg, Section XG)

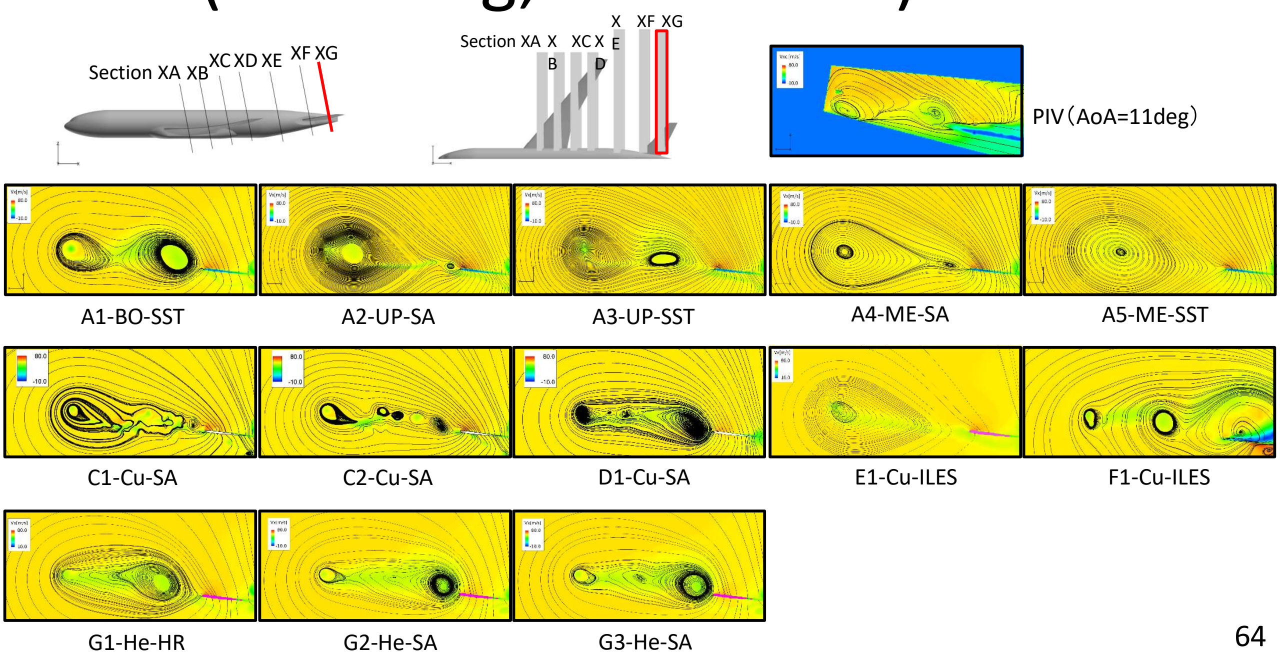

64

Velocity contours (13.08deg, Section XA)

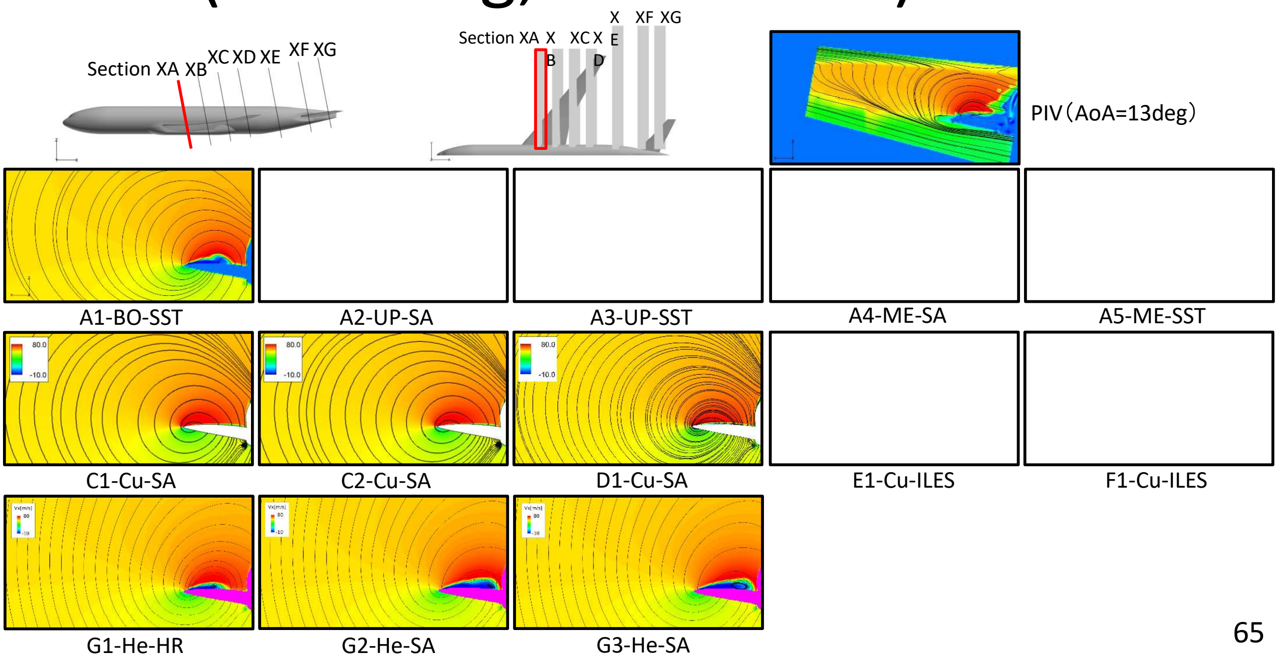

65

Velocity contours (13.08deg, Section XB)

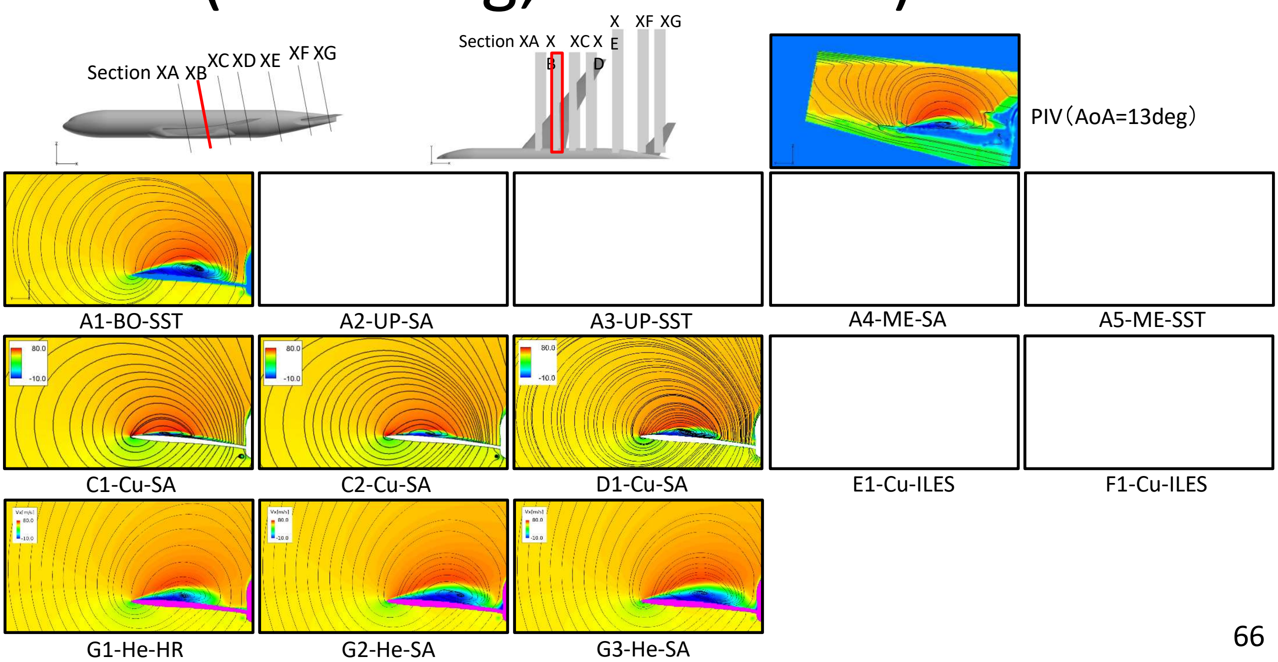

66

Velocity contours (13.08deg, Section XC)

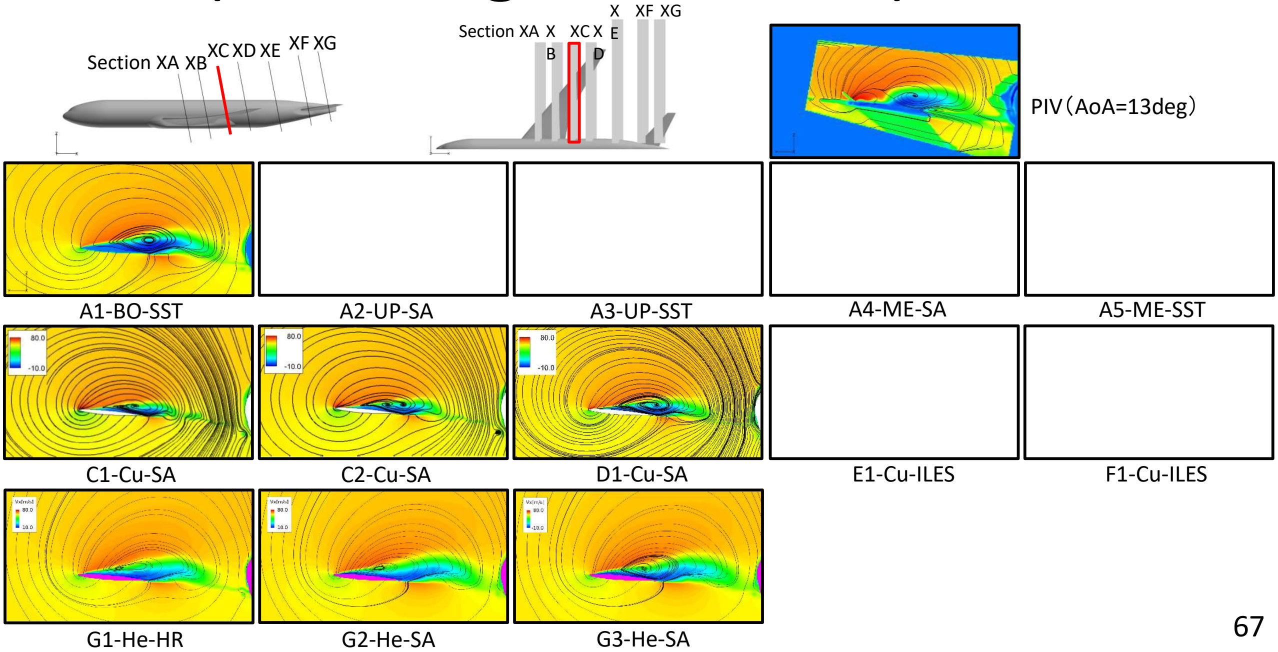

67

Velocity contours (13.08deg, Section XD)

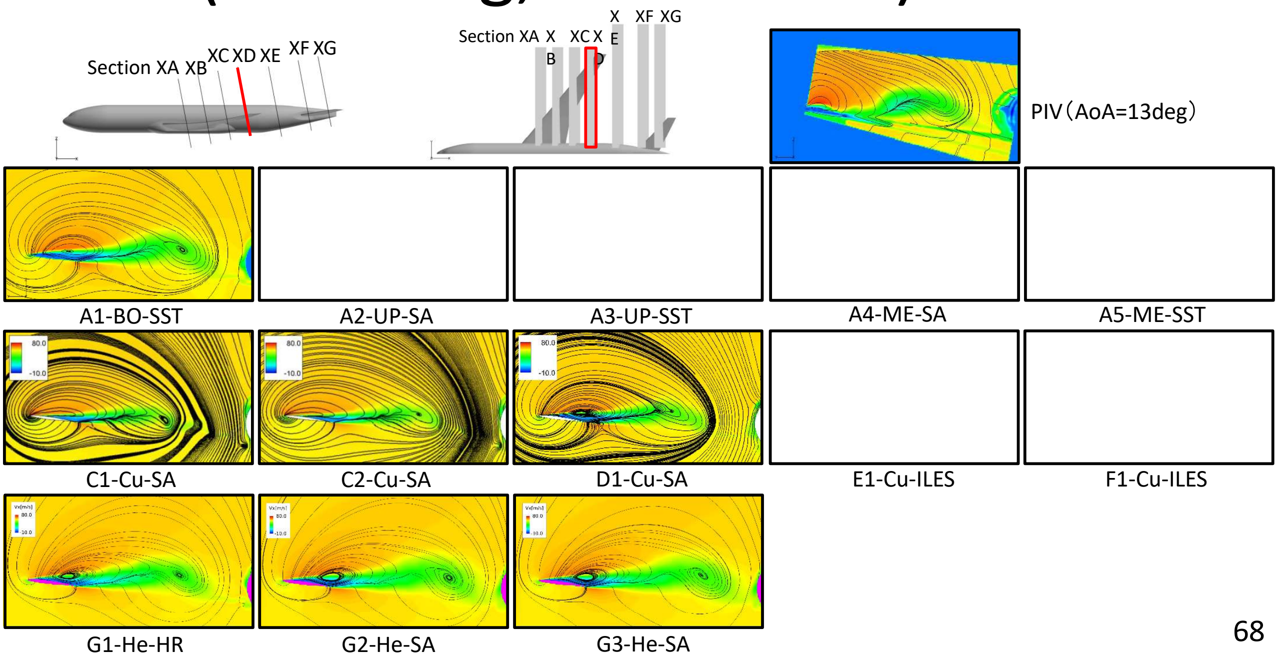

68

Velocity contours (13.08deg, Section XE)

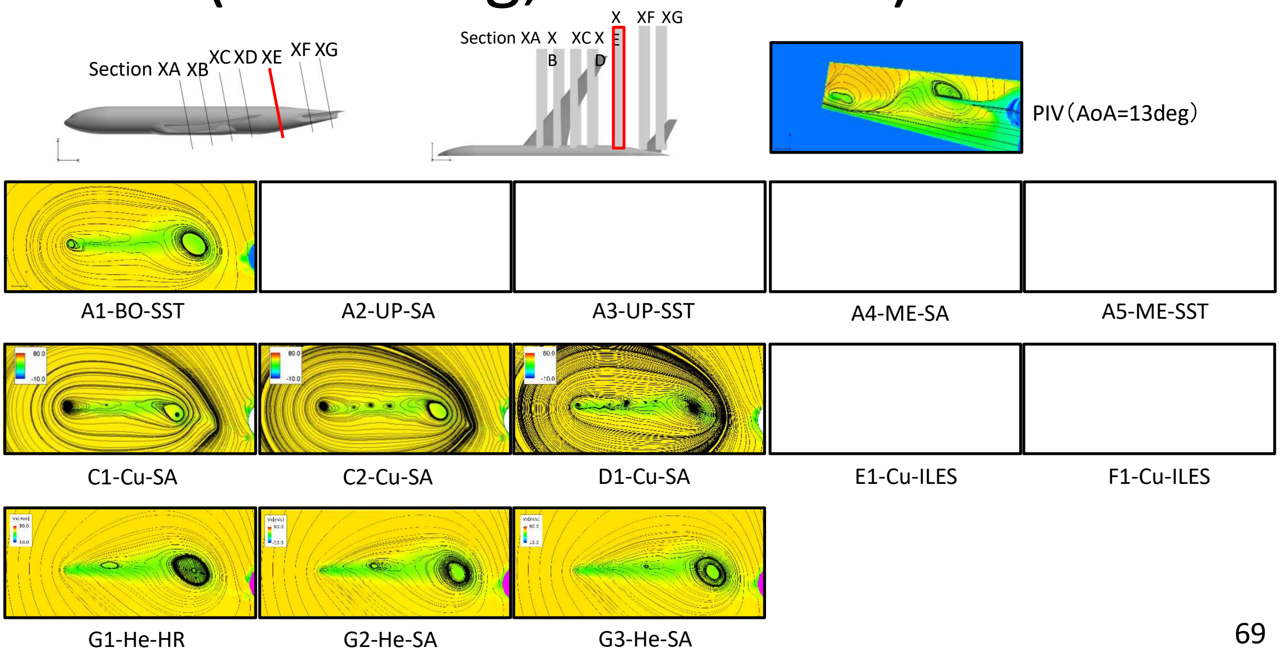

69

Velocity contours (13.08deg, Section XF)

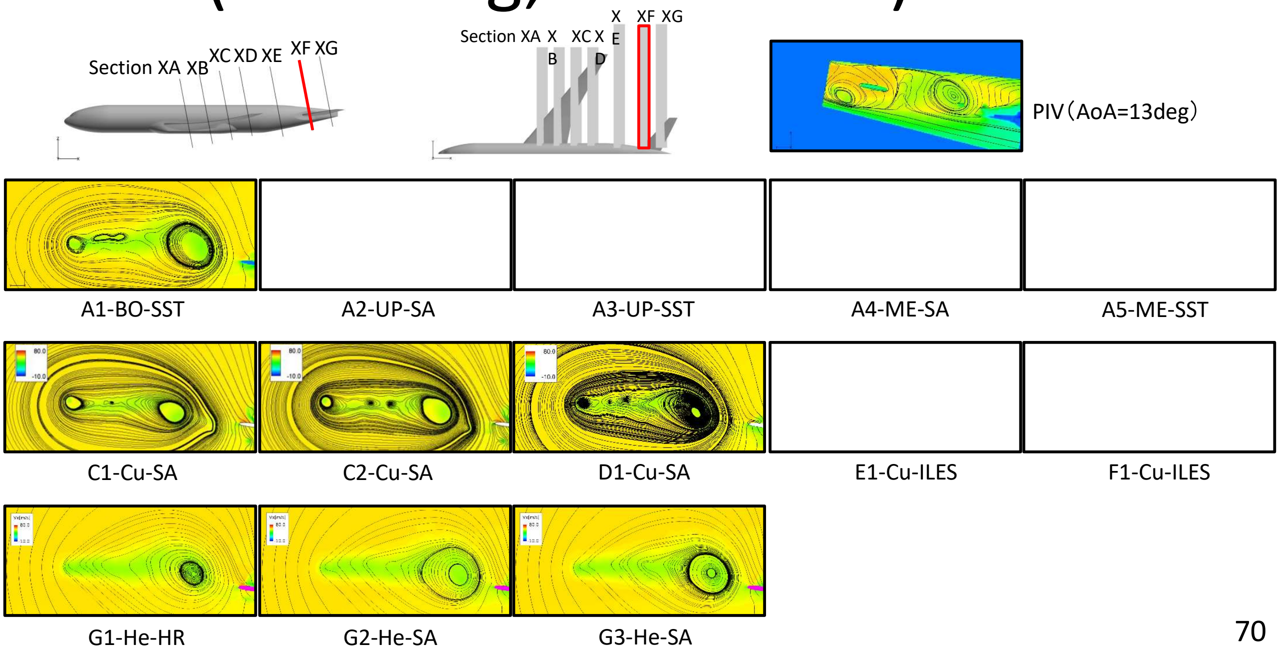

70

Velocity contours (13.08deg, Section XG)

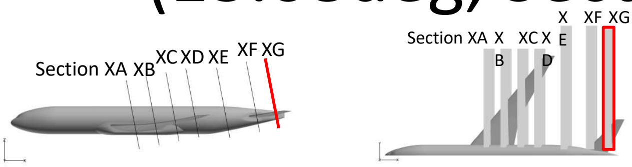

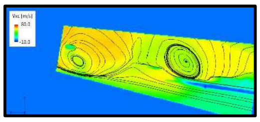

PIV（AoA=13deg）

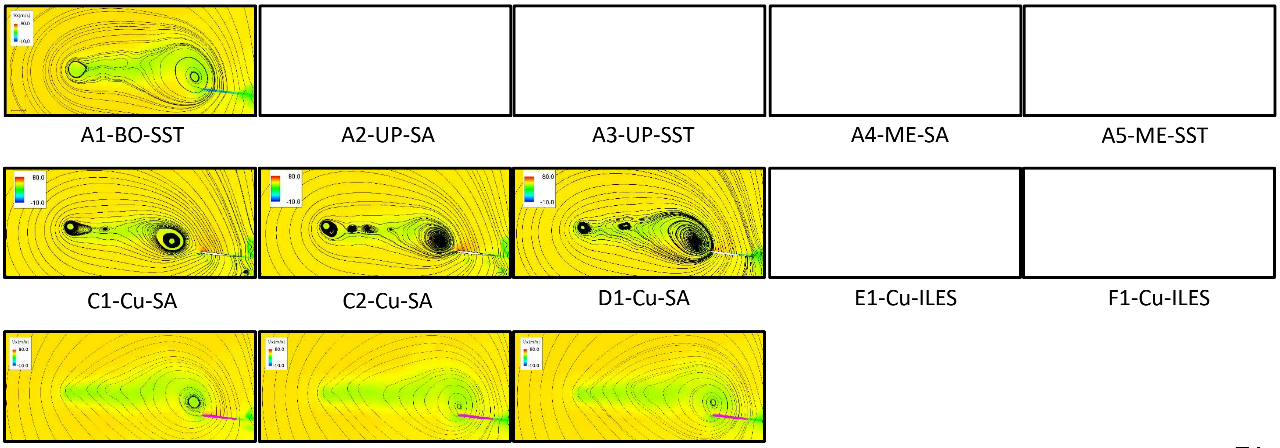

A1-BO-SST	A2-UP-SA	A3-UP-SST	A4-ME-SA	A5-ME-SST
C1-Cu-SA	C2-Cu-SA	D1-Cu-SA	E1-Cu-ILES	F1-Cu-ILES
G1-He-HR	G2-He-SA	G3-He-SA		

Surface Cp distribution（Tail, Section HB-HC）

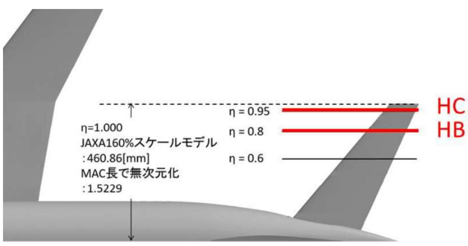

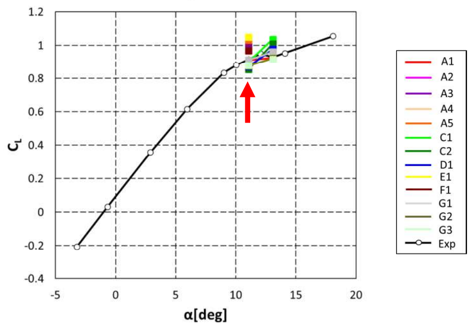

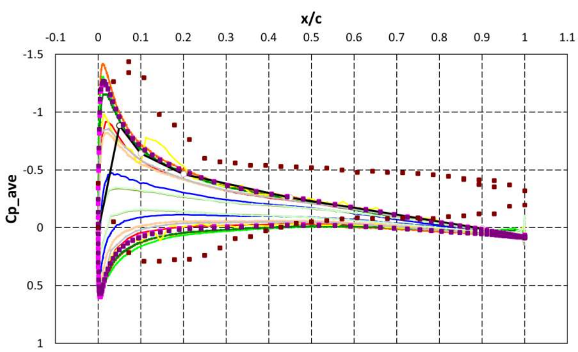

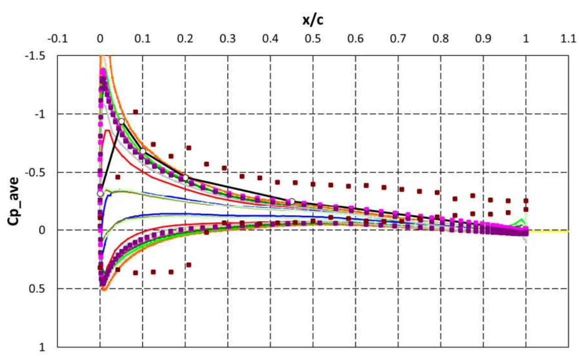

Surface Cp distribution（Tail, Section HB-HC）

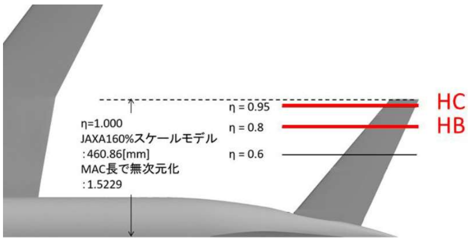

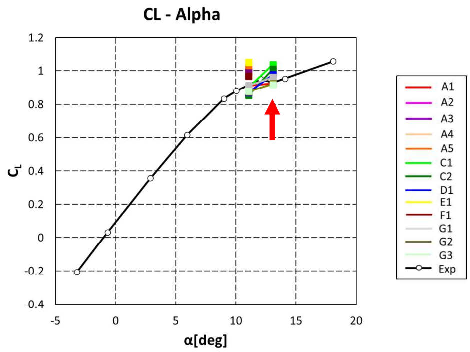

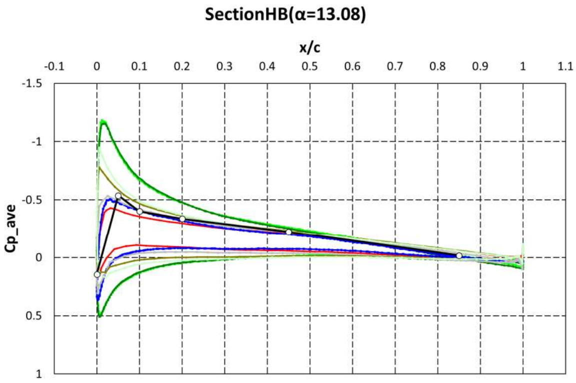

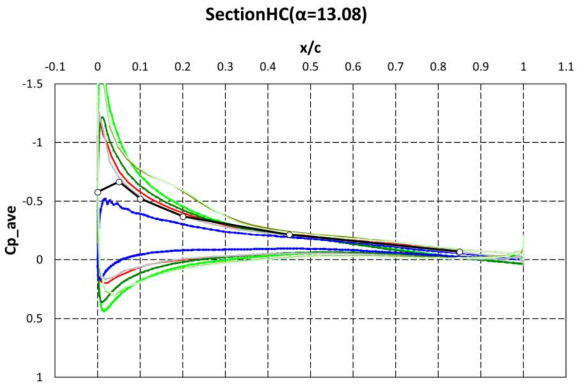

Surface Cp distribution（Tail, Section HB-HC）

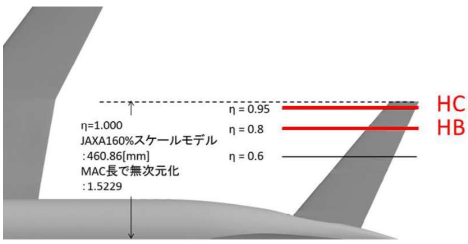

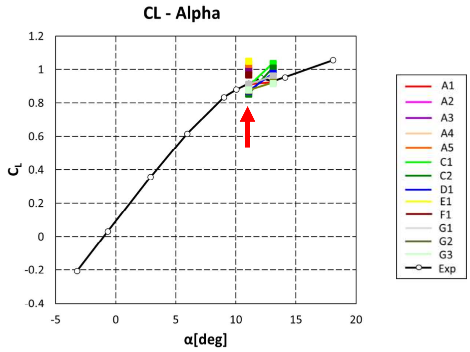

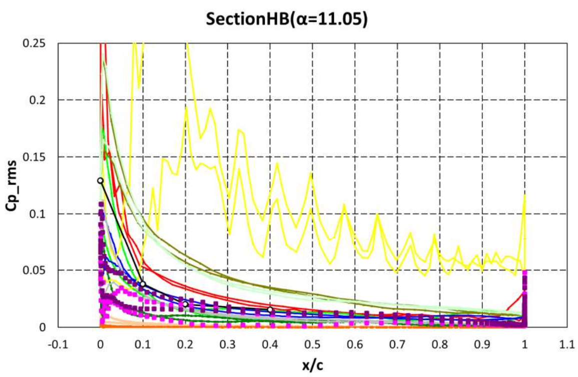

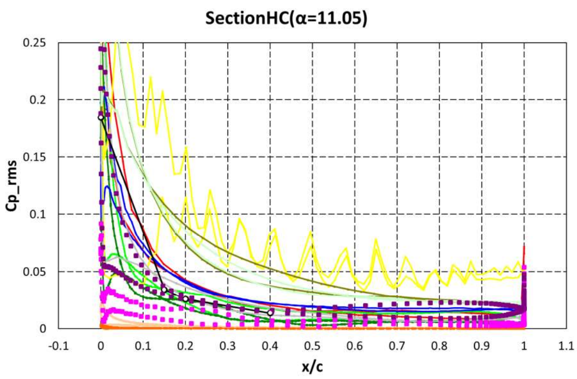

Surface Cp distribution（Tail, Section HB-HC）

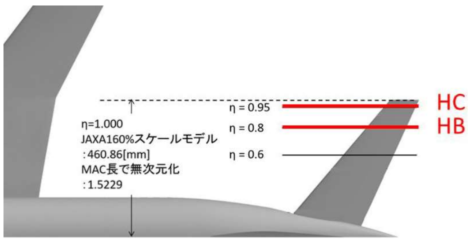

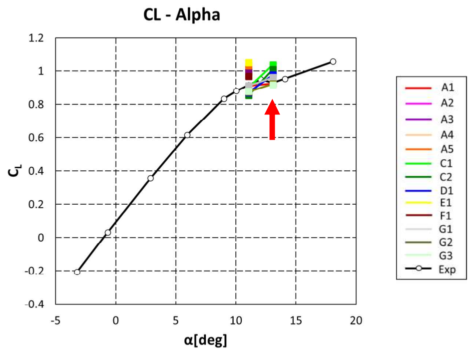

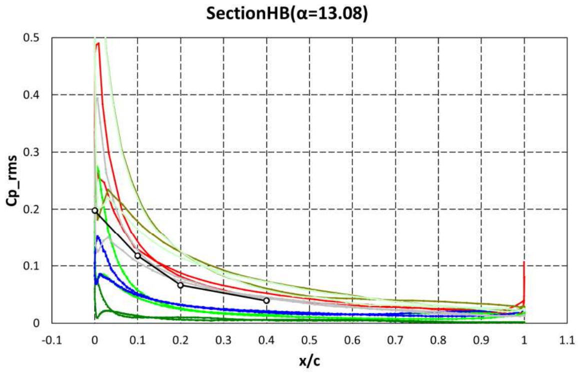

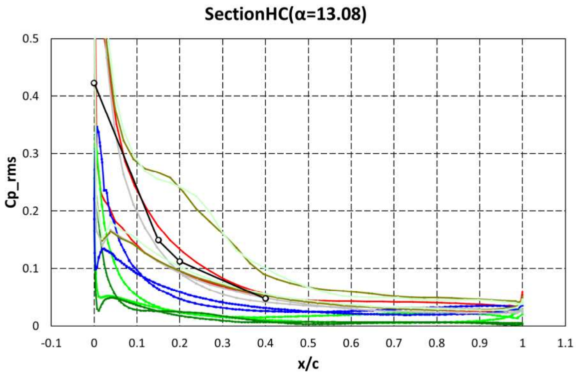

75

Surface Cp distribution（Main wing, Section B’-D’）

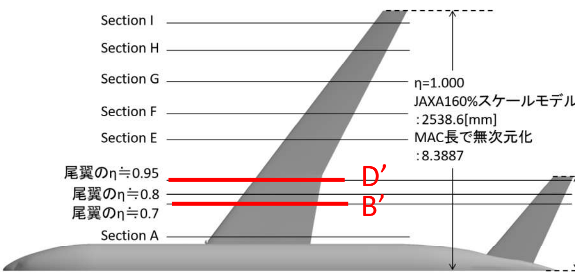

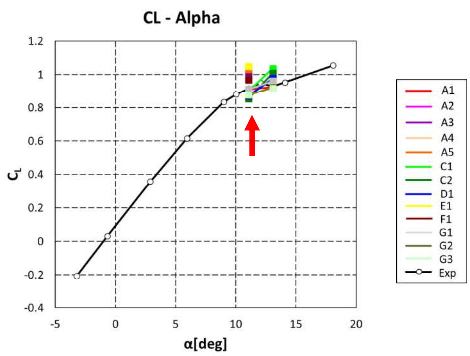

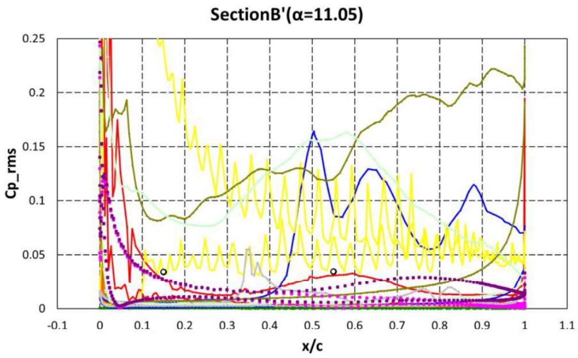

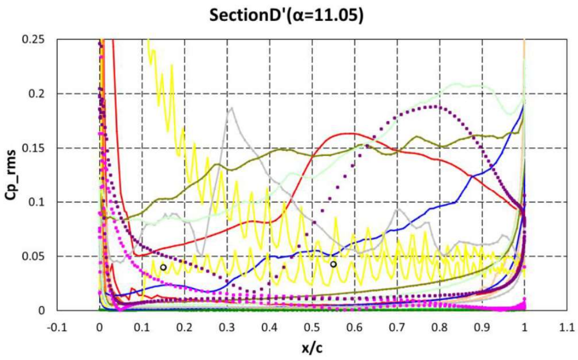

76

Surface Cp distribution（Main wing, Section B’-D’）

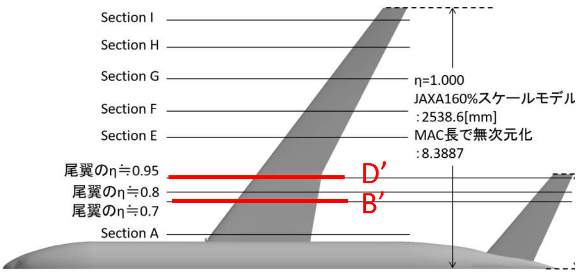

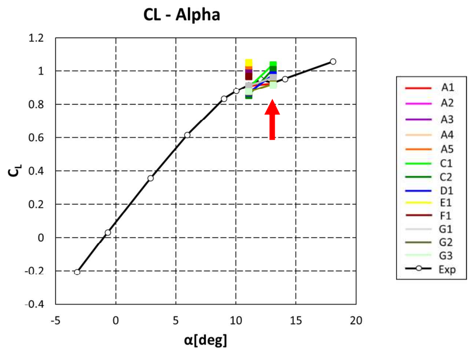

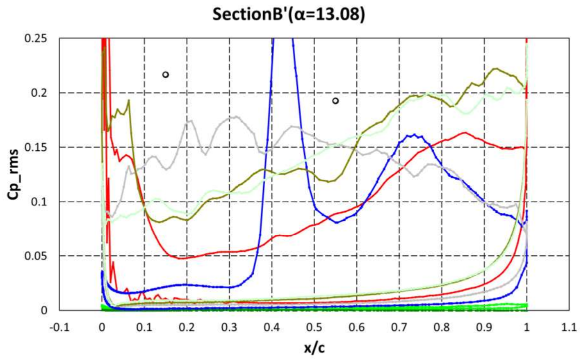

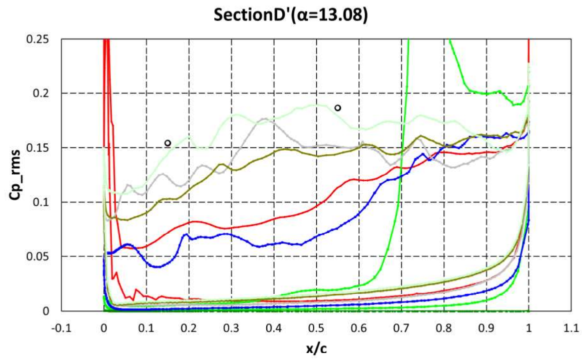

Summary

- The stall prediction is affected by the grid type (hexahedral/mixed-element unstructured grid, structured grid) and the boundary treatment (body-fitted grid, immersed boundary).
- The SST model predicts the stall at lower angle of attack than the SA model for various grids.
- The prediction of mild and partial separation that appears at 11deg is very challenging. The prediction of large separation at 13deg is improved by using the unsteady simulation. The variation of the predicted lift is reduced as compared with APC-6.
- The wake is diffused for the mixed-element grid that is relatively coarse between the main wing and the tail. However, for the other grids, the effect of the grid resolution on the wake profile is not clear since the wake profile is largely affected by the main wing separation.
- The rich PIV data enabled the detailed validation of three-dimensional separated flow.